ABSTRACT

CHEMISTRY

MITCHELL, ALESIA SAWYER **B.S., CLARK COLLEGE, 1989**

A SEMIEMPIRICAL (AM1) STUDY OF THE REACTIVITY OF REDOX STATES OF QUINONE-CONTAINING MODEL SYSTEMS FOR ANTHRACYCLINE PHARMACOPHORES

Advisor: Yitbarek H. Mariam, Ph.D.

Thesis dated December, 1993

The reactivity of redox states of model systems for anthracycline pharmacophores were examined by the AM1 semiempirical approach. The redox states examined were quinone (Q), quinone radical anion ($Q^{-\cdot}$), semiquinone radical ($QH^{\cdot}$), semiquinone anion (QH^{-}), and hydroquinone (QH_2), while the model systems were 1,4-benzoquinone (I), 1,4-naphthaquinone (II), hydroxy-naphthaquinone (III) and dihydroxy-naphthaquinone (IV), which are all part of the pharmacophores of several anthracyclines. The imine and/or diimine derivatives of 1,4-benzoquinone and dihydroxy-naphthaquinone were also investigated. The relative reactivity of Q, $Q^{-\cdot}$, $QH^{\cdot}$, QH^{-}, and QH_2 were examined by utilizing absolute electronegativity and chemical hardness data. In all cases, $Q^{-\cdot}$ and QH^{-} were found to be the most reactive species suggesting that these redox states are probably the ones that transfer their electrons to molecular oxygen thereby generating reactive oxygen species. The imine and diimine analogs were shown to have higher reactivity. This strongly suggests

that 5-iminodaunomycin, a C-5 imine derivative of daunomycin, which has been described as redox-incapacitated, should not be less reactive than daunomycin. Based on electronegativity data, there were no specific reactivity trend observed for redox states of the four quinone systems (I-IV); however, absolute hardness data suggested that $Q^{\cdot-}$ was the most reactive intermediate for all four systems. SOMO and LUMO energies, absolute electronegativities and chemical hardness values, and reaction enthalpies (for the electron attachment to Q) of 12 disubstituted naphthaquinones were also correlated with their experimental reduction potentials using a least squares analysis. When all 12 points were included, the correlation coefficients obtained were: 0.28 (SOMO energies), 0.40 (LUMO energies), 0.41 (absolute hardness), 0.53 (electronegativity), and 0.57 (reaction enthalpies). In all cases, exclusion of three points gave better correlations with coefficients in the range of 0.73-0.91. In general, SOMO and LUMO energies and reaction enthalpies decreased with increasing reduction potential and absolute hardness and electronegativity values increased with increasing reduction potential. Since experimental reduction potentials have been shown to correlate with antitumor activity, this study shows the various electronic properties considered in this study should also correlate with antitumor activity, and thus can be used to generate a data base for structure-activity correlations and for new drug design purposes.

A SEMIEMPIRICAL (AM1) STUDY OF THE REACTIVITY OF REDOX STATES OF QUINONE-CONTAINING MODEL SYSTEMS FOR ANTHRACYCLINE PHARMACOPHORES

A THESIS

SUBMITTED TO THE FACULTY OF CLARK ATLANTA UNIVERSITY

IN PARTIAL FULFILLMENT OF THE REQUIREMENTS FOR

THE DEGREE OF MASTER OF SCIENCE

BY

ALESIA SAWYER MITCHELL

DEPARTMENT OF CHEMISTRY

ATLANTA, GEORGIA

DECEMBER 1993

ACKNOWLEDGEMENTS

The author would like to express her gratitude and appreciation to her research advisor, Professor Yitbarek H. Mariam for his guidance, understanding, encouragement, and extreme dedication to the completion of this investigation and thesis. The author would also like to thank Dr. Roosevelt Thedford, Dr. Alfred Spriggs and Dr. Bonita Alick for their support and encouragement throughout her undergraduate and graduate career. The author thanks, Dr. John Browne for moral, and the MBRS Program for financial support throughout her stay at Clark Atlanta University. The author also thanks Mrs. Deborah Steward for her help in finalizing the format of this paper. Finally, the author wishes to dedicate this thesis to her mother, Mrs. Bertha Sawyer, brother, Mr. Michael Daniel, late sister, Miss. Kimberly M. Sawyer and husband, Mr. Willie R. Mitchell. May God bless and watch over you in all your endeavors.

NOTICE TO BORROWERS

All dissertations and theses deposited in the Robert W. Woodruff Library must be used only in accordance with the stipulation prescribed by the author in the preceding statement.

The author of this thesis is:

Name: Alesia Sawyer Mitchell

Street Address: 3585 Cameron Hills Place

City, State and Zip: Ellenwood, GA 30049

The director of this thesis is:

Professor: Dr. Yitbarek H. Mariam

Department: Chemistry

School: Arts & Sciences

CLARK ATLANTA UNIVERSITY

Office Telephone: 880-8593

Users of this thesis not regularly enrolled as students of the Atlanta University Center are required to attest acceptance of the preceding stipulations by signing below. Libraries borrowing this thesis for use of patrons are required to see that each user records here the information requested.

NAME OF USERS	ADDRESS	DATE	TYPE OF USE

TABLE OF CONTENTS

LIST OF TABLES

LIST OF FIGURES

I. INTRODUCTION

Quinoid compounds are widely distributed in nature. They can be found in bacteria, fungi, higher plants in the animal kingdom, in arthropods, echinoderms, and as components of the respiratory system in humans.[1] Quinoid compounds containing oxygen are called quinones. There are three major groups of naturally occuring quinones. These include benzoquinones, napthoquinones, and anthraquinones. The later class, anthraquinones, when extensively substituted, are clinically useful anticancer agents.[1]

Within the anthraquinones class, anthracycline glycosides represent the largest class of clinically useful antineoplastic quinoids. They were first investigated in the late 1950's as pigmented antibiotics produced by different strains of Streptomyces.[2] The era of antitumor anthracyclines began with the isolation of daunomycin from Streptomyces peucetius in 1963,[3] followed by the isolation of its derivative, adriamycin in 1967 from mutant strains of Streptomyces called Streptomyces peucetius var. caesius.[4]

Active anthracyclines are composed of a tetracyclic quinone-containing aglycone chromophore linked, to a monosaccharide carbohydrate chain known as daunosamine. Several of the biological effects of anthracyclines are presumed to be derived from the quinone moiety acting as an oxidant.[5] Out of approximately twenty anthracyclines, tested clinically and experimentally, daunomycin and adriamycin are by far the most widely used agents.[6] Daunomycin, also known as daunorubicin, and adriamycin, known as

doxorubicin, are structurally similar anthracyclines which differ from each other by a hydroxyl group located on the C-14 position of the tetracyclic moiety (Figure 1).

Three major pathways have been identified as major mechanisms by which anthracyclines are metabolized. These pathways are keto reduction, cleavage reactions, and conjugation.[7] Keto reduction involves the C-13 ketone moiety on the drug molecule being reduced to a C-13 alcohol derivative. This takes place in the presence of a soluble enzyme known as $NADP^+$ oxidoreductase and a NADPH coenzyme.[7] Reductive cleavage (at the C-7 position) of anthracyclines involves the loss of the carbohydrate chain thereby forming inactive aglycones. This reaction takes place in the presence of NADPH-cytochrome P-450 reductase. The last metabolic pathway in anthracycline metabolism is conjugation. This pathway involves the formation of glucoronide and sulfated conjugates.[7] Even though these three metabolic pathways are important for the understanding of the metabolism of this class of drugs, radical and quinone methide formations are by far the most studied mechanisms because of postulated chemotherapeutic and toxicological effects.[8] Daunomycin's and adriamycin's major metabolites have been found to be daunorubicinol and doxorubinol, respectively.[9] These metabolites account for up to 50% of the major metabolites, followed by the unchanged drug and polar metabolites. Figure 2 displays several metabolic pathways by which anthracyclines undergo, along with their corresponding metabolites.[9]

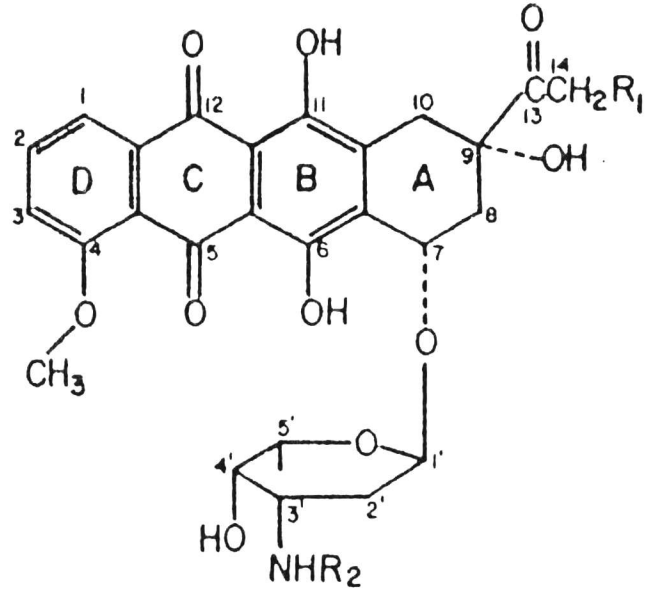

$R_1, R_2 = H$ Daunomycin, 1

$R_1 = OH, R_2 = H$ Adriamycin, 2

Figure 1. Structures of daunomycin and adriamycin.

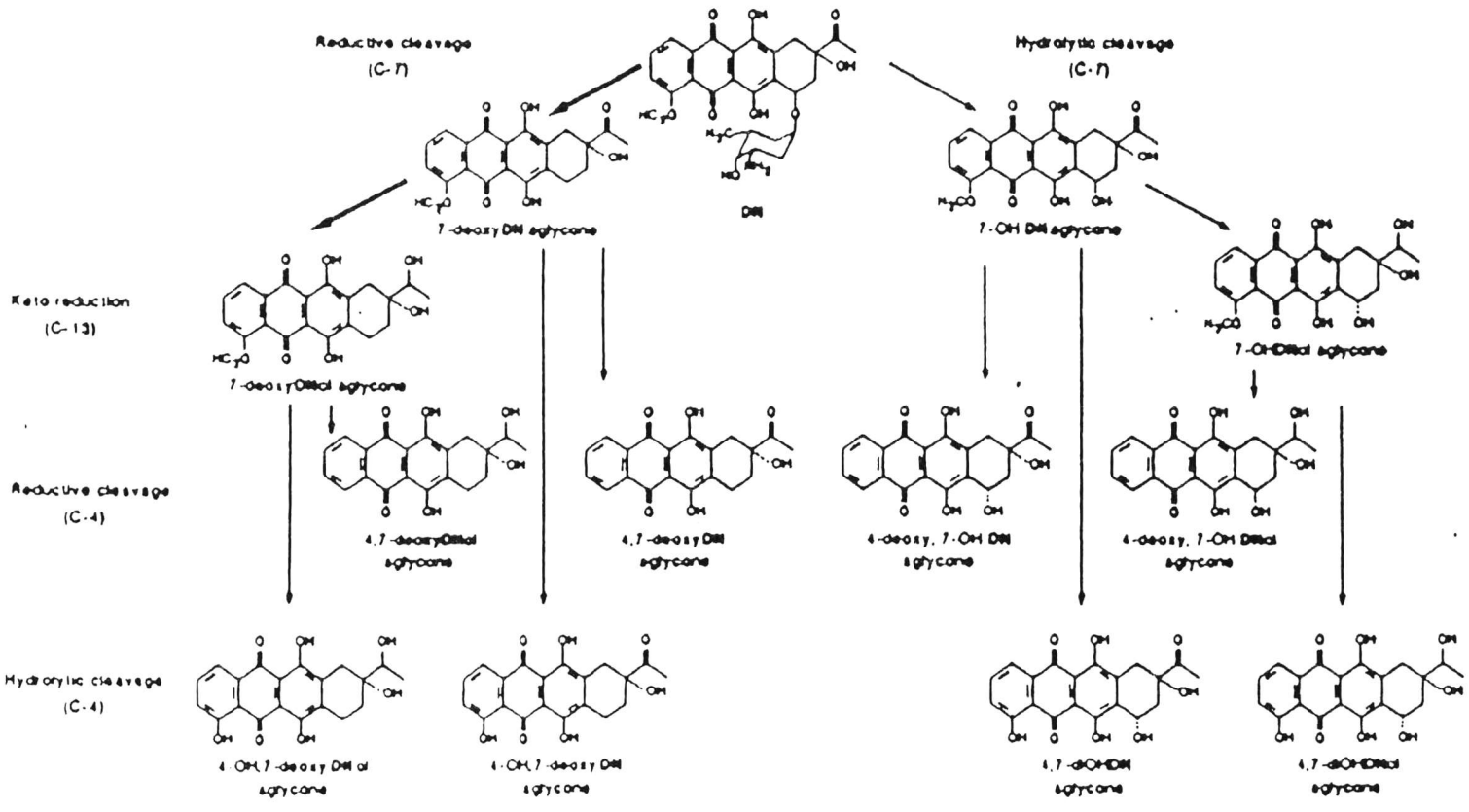

Figure 2. Metabolic pathways of anthracyclines.

The most potent reducing agent for formation of anthracycline metabolites is the microsomal NADPH cytochrome P450 reductase.[10] However, other enzymatic reducing agents have been utilizrd to reduce anthracyclines. They are xanthine oxidase, NADPH ferredoxin oxidoreductase, and NADH cytochrome C reductase.[11] Chemical reagents, capable of reducing the anthracycline class of drugs, include sodium borohydride, sodium dithionite, dimethyl sulfoxide, and 3,5,5,-trimethyl-2-oxomorpholin-3-yl. All have been proposed to donate one electron to the drugs.[12]

Both daunomycin and adriamycin have generated considerable interest because of their outstanding clinical utility as anticancer drugs. Daunomycin and adriamycin have demonstrated effectiveness against various leukemias. These include: acute granulocytic and lymphocytic leukemias, Hodgkin's and non-Hodgkin's lymphomas, and neuroblastoma.[3,13] In addition, adriamycin has been shown to be effective against the carcinoma of the breast, bronchogenic carcinoma, ovarian carcinoma, soft tissue sarcoma.[14]

Although both chemotherapeutic agents have displayed high efficacy and importance in the treatment of a wide variety of neoplasmas, they are characterized by a number of undesirable adverse side effects which have greatly limited their uses. Toxic effects include: myelosuppression, nausea, vomiting, hair loss, and most seriously, cardiomyopathy, a cumulative dose-dependent side effect.[15]

Cardiotoxicity of the anthracycline antitumor agents was first described for

daunomycin.[16] Since adriamycin isolation and clinical investigation, researchers have demonstrated that adriamycin has about twice the cardiotoxicity as daunomycin.[17] Zweier and co-workers observed that adriamycin is complexed and oxidized by aqueous iron(III),[18] while daunomycin forms a complex with iron(III) but is not oxidized. They proposed that oxidation of the C-14 hydroxyl group of adriamycin can occur and that its increased toxicity is related to radically produced products of that oxidation. The oxidation products have been isolated by Gianni.[19]

Three clinical manifestations of cardiac-toxicity have been observed. These include acute dysrhythmias, semiacute myocarditis, and the most serious cardiotoxicity, a chronic cumulative disease that can result in heart failure. Impairment of the mitochondrial function in myocardiac cells have been proposed to be responsible for cardiotoxicity.[20] As a result of this, both daunomycin and adriamycin have been the focus of intensive chemical and biological investigations since their discovery.

Most investigators believe that anthracycline cytotoxicity is a result of several biological pathways and that full expression of an anthracycline antitumor activity may represent one or more proposed mechanisms.[21] The first studied mechanism is the high affinity binding of anthracyclines to DNA through intercalation.[22] DNA intercalators are generally polycyclic planar compounds that bind double-stranded DNA by inserting between base pairs, resulting in partial unwinding of the DNA molecule around the intercalation

site.[23] Anthracyclines have been shown to inhibit DNA and RNA synthesis by binding to the nucleic acids and disrupting the enzymatic reaction. Daunomycin, for example, has been shown to inhibit DNA directed RNA synthesis by inhibitng E. coli RNA polymerase in vitro.[24]

A number of experimental researchers have used various techniques to examine the intercalation process. These techniques include hydrodynamics, calorimetry, spectroscopy, and X-ray diffraction.[25-28] These techniques have shown that these molecules interact with double-stranded nucleic acids through non-covalent intercalation of their chromophore between adjacent base pairs in the DNA double helix. This leads to blockage of DNA, RNA and protein synthesis, DNA protein-associated strand breakage and inhibition of DNA repair.[29]

Crothers et. al. demonstrated that the intercalation of anthracyclines in DNA is an exothermic process with a perference for binding to the guanine-cytosine base pairs.[30] Sinha has provided evidence which indicates that covalent binding of anthracyclines to DNA and proteins occurs under anaerobic conditions.[31] Minor modes of DNA binding to the anthracycline antibiotics have included associations at high drug levels, involving electrostatic and hydrogen bonds. These interactions are presumed to occur, to a large extent, at the exterior site of the DNA double helix (Figure 3).[32] The equilibrium interaction of adriamycin and it's N-acetyl derivatives, demonstrated that a series ofpurine-pyrimidine alternating polydeoxyribulose, were studied using spectroflurometry to assess

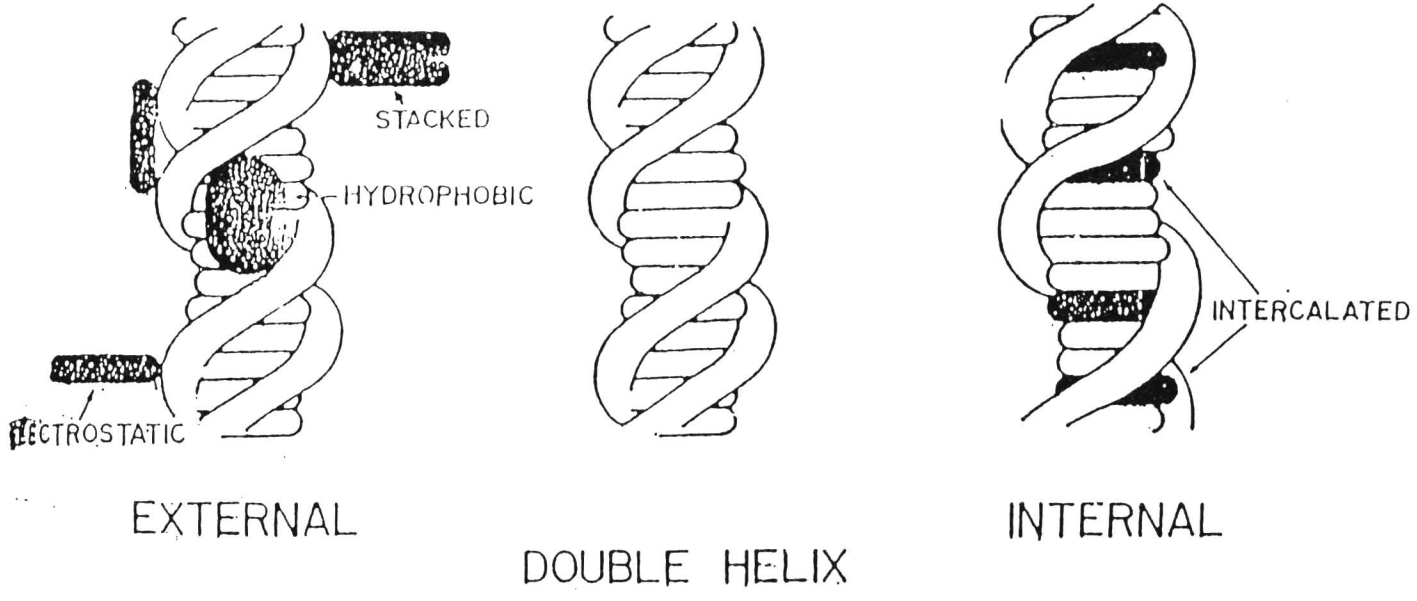

Figure 3. Binding of planar drug moieties into the DNA molecule

the relevance of the electrostatic contribution to DNA interaction. Results indicate that supression of the positive charge on the aminosugar have a profound negative effect on the free energy of intercalation and a negligible influence on the base specificity.

Another proposed mechanism, for cytotoxicity of the anthracyclines has focused on cell membrane effects.[33] Anthracyclines have been shown to bind to the cell membrane. This results in membrane damage which alters membrane fluidity and altered ion permeability, glycoprotein synthesis changes, phospholipid structure changes and protein transport alterations.[34] These can, consequently, result in altered permeability to the Ca^{+} ion.[35]

The last proposed mechanism for cytotoxicity involves reactive radical metabolites. Anthracyclines are beleved to be bioreductively-activated to semiquinone, hydroquinone, and quinone methide metabolites, through one-elecron reductions.[36] The two most popular schemes for the redox-mediated cytotoxicity involve the formation of reactive oxygen species displayed in Figure 4 and the production of quinone methides, reactive aglycon tautomers presumably capable of covalently binding to a variety of biological molecules as displayed in Figure 5.

Thus far, general background information has been given to provide a basic overview of the anthracycline antibiotics. In upcoming sections, emphasis on radical formations, quinone methide formation, and cardiotoxicity will be discussed based on past and recent investigations done so far.

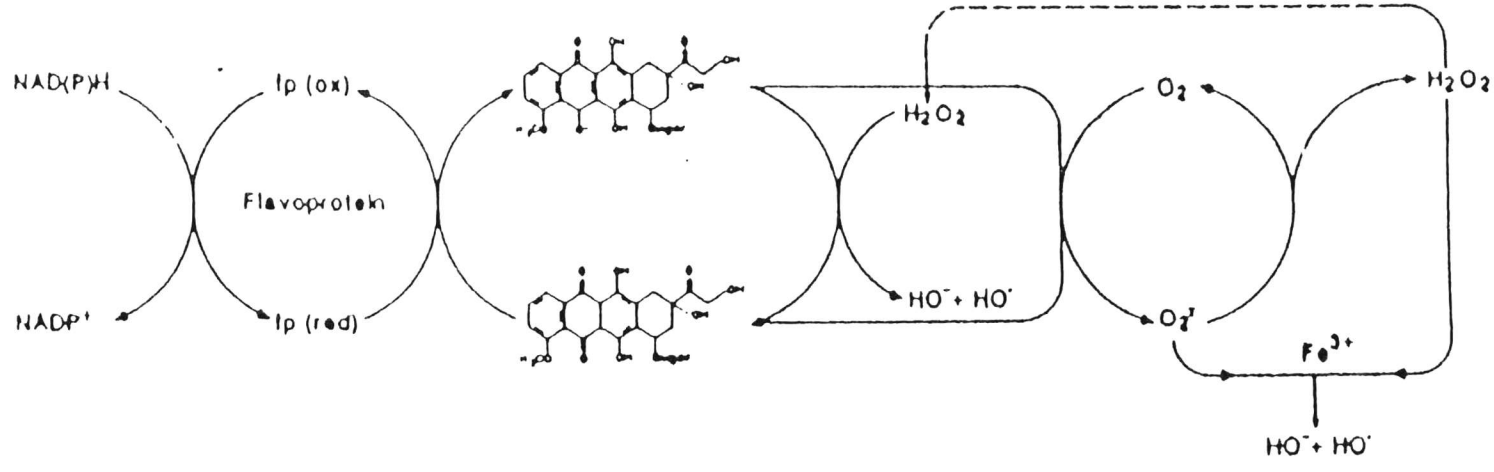

Figure 4. Formations of reactive oxygen species.
(Taken from Powis, G.; Prough, R. A. "Metabolism & Action of Anticancer Drugs" 1987, London Press, pp.211)

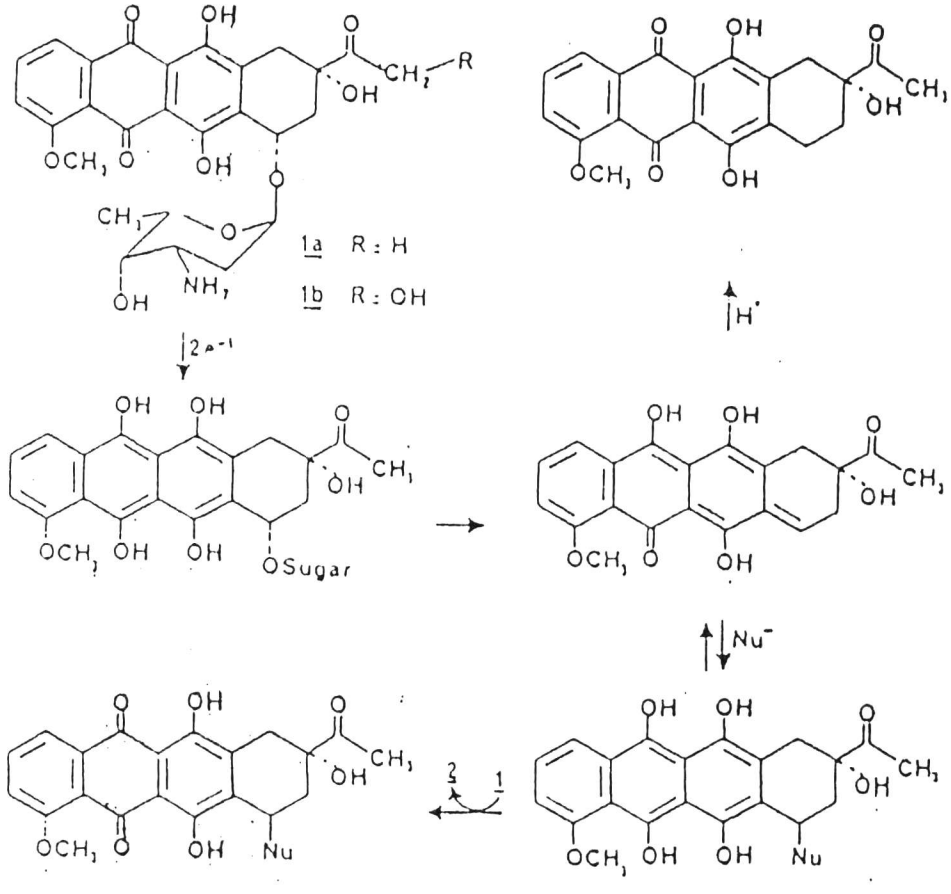

Figure 5. Proposed mechanism for the production of quinone methide.
(Taken from Ramikrishman, K.; Fisher, J. J. Med. Chem. 1986, 29, 1215.)

A. Radical Formation

Daunomycin and adriamycin have been demonstrated to efficiently catalyze the production of reactive oxygen species by transfering one- or two- electron reduced products to molecular oxygen.[37] Formation of the reactive oxygen species in vivo is generally considered to be an aerobic process in which a single electron transfer leads to the formation of the anthracycline semiquinone radical. The anthracycline semiquinone radical subsequently transfers unpaired electron (radical) to oxygen, leading to the formation of reactive oxygen species (i.e. superoxide radical), which can eventually lead to the formation of hydrogen peroxide, and hydroxyl radical.[37] All these species have been shown to inflict oxidative stress by attacking heart cell membrane lipids. This has been demonstrated by the quinone moiety undergoing flavoenzyme catalyzed one-electron reduction to form radicals.[37] In 1975, investigators first reported that daunomycin and adriamycin when incubated with rat liver microsomes and NADPH (under aerobic conditions) formed radicals that were capable of inducing the formation of superoxide radical anions.[38] Bachur et al[39] demonstrated single electron reduction of several quinone-containing drugs to a free radical state by microsomal NADPH cytochrome P-450 reductase, and stimulation of NADPH-dependent microsomal oxygen consumption by anthracyclines. They identified the free radical intermediate as semiquinone radical, which functions as an electron carrier transferring its electron to molecular oxygen.

Electron spin resonace (esr) spectroscopy has been used to detect semiquinones of daunomycin and adriamycin.[40] Sato et al. reported esr spectra of anthracycline semiquinone radicals when the drugs were incubated with NADPH rat liver microsomes.[40] High resolution esr was used to differentiate adriamycin and daunomycin semiquinone formation using xanthide/xanthide oxidase.[41] The properties of semiquinone radicals have also been studied by pulse radiolysis.[42] Results show that daunomycin and adriamycin semiquinone free radicals react rapidly with molecular oxygen with the reaction rate constant being bimolecular ($3x10^8 M^{-1}s^{-1}$).

The oxygen species formed by reaction of molecular oxygen with the anthracycline semiquinone has been shown to be the superoxide anion radical. Formation of this radical has been demonstrated by chemical assays and by esr studies using dimethyl-1-pyrroline-1-oxide (DMPO) to spin trap the superoxide anion radical as a stable adduct.[43]

Superoxide anion radical has been speculated to react with anthracycline to give rise to biologically important reactive intermediates.[44] One study showed the interaction of superoxide anion radical with daunomycin and its aglycones in aprotic media. Results revealed that the superoxide anion radical can extract a proton from one of the phenolic groups to generate its anion analog.[45] The analog consequently is reoxidized by molecular oxygen and the species responsible for the biological activity is produced.

The superoxide anion formed by redox-cycling (production of reductively

activated species) of anthracyclines can give rise to a hydroxyl radical that leads to degradation of deoxyribose and to breakage of DNA strands.[46] This process involves the superoxide anion being catalyzed by a iron salt reaction that yields the production of hydroxyl radicals. Hydroxyl radicals can also be formed by the immediate reaction of the semiquinone radical (reduced intermediate of anthracyclines) with hydrogen peroxide. Winterbourne et al first demonstrated this process which occured under aerobic conditions.[47] The method involved using the ESR technique of spin-trapping to detect daunomycin-dependent superoxide and hydroxyl radical formation.

B. Quinone Methides Formation

The chemistry of anthracycline quinone methides has been studied intensively because quinone methides are proposed as possible reactive forms to covalently bind biological molecules. This binding occurs with proteins, lipids, and DNA. In the absence of molecular oxygen, species formed as a result of reduction can undergo elimination of the sugar group, daunosamine, to give the quinone methide.[48] In Figure 5, the proposed mechanism for this process is visualized by one and two-electron reduction of the anthracycline. One-electron reduction of daunomycin and adriamycin with limited amounts of sodium borohydride under anaerobic conditions[49] or reduction by NADPH rat liver under aerobic and anaerobic conditions results in the covalent binding of anthracycline to microsomal proteins and to the DNA molecule.[50]

Two-electron reduction of adriamycin with excess sodium borohydride can

also result in covalent binding of anthracyclines to DNA.[51] This process has been demonstrated in reconstituted systems of adriamycin, cardiolipin, mitochondrial NADH-cytochrome c reductase and NADH.[48]

The minimal requirements for the production of quinone methide are anaerobicity (a non-oxygen environment), an enzyme catalyst to mediate anthracycline reduction, and a suitable reducing agent. Moore first proposed a mechanism for activation of anthracyclines involving two-electron reduction to the anthracycline hydroquinone hence giving the quinone methide. This process involves the C-7 sugar group (monosacharide carbohydrate) being converted from a stable functional group to a stable leaving group in the hydroquinone portion of the molecule.[52]

Koch and Fisher have demonstrated that anthracycline quinone methides can react with electrophiles and nucleophiles.[53] Electrophilic attack by a proton restores the quinone chromophore while nucleophilic attack yields a hydroquinone adduct, which can eliminate the nucleophile to reform the quinone methide unless it is oxidized to a quinone adduct. Ramarkrishnan and Fisher have reported electrophilic addition of daunomycin activated by spinach NADPH:ferredoxin oxidoreductase and NADPH to thiol nucleophiles such as N-acetylcysteine thus providing evidence for catalytic hydroquinone adduct formation.[54]

Treatment of MCF-7 cells with adriamycin in the presence of purified rat NADPH cytochrome P450 reductase (flavoprotein enzyme in the microsomes)

and NADPH resulted in a marked enhancement of the drug's cytotoxicity. The data suggest that oxygen radicals do not play a primary role in the enzymatic-mediated adriamycin cytotoxicity and that the mechanism of toxicity involves a reactive species which binds to cellular nucleophiles.[55]

In the absence of a reactive macromolecule or small molecule substrate, the quinone methide tautomerizes to the 7-deoxyaglycon of the anthracyline which is an important metabolite. Mechanistic studies of the reduction of 4 anthracyclines: 11-deoxydaunomycin, adriamycin, 4-demethoxydaunomycin, and demethoxy-6-deoxydaunomycin with TM-3 dimer has been demonstrated.[56] TM-3, a mild one-electron reducing agent for anthracyclines, has proven to be a useful reagent for the sequential generation of many redox states. In particular, the quinone methide states of the first 3 antibiotics from glycosidic cleavage of their respective hydroquinone states were chacterized and the rate constants for the tautomerization to their 7-deoxyaglycons were determined.[56] The last anthracycline hydroquinone state reacted via hydride to oxazinone and was shown to be stable with respect to the glycosidic cleavage. Quinone methide intermediates from glycosidic cleavage of the first three agents were studied by UV-Vis spectroscopy and the rate constants for their tautomerization to their respective 7-deoxyaglycons were determined.

C. Cardiotoxicity

Congestive heart failure cardiotoxicity, related to the anthracycline class of drugs, consists of a cumulative toxicity to the myocardial fibrils which

produces myofibrilar loss. Loss of the myofibrillar consequently leads to an inadequate pumping of the heart.[57] Toxic effects of free radicals on the heart have been implicated for this cardiotoxicity.[58] Other mechanisms have also been suggested to account for the cardiotoxicity of anthracyclines. These include ability of anthracyclines to delocalize iron from cardiac ferritin stores, disturbances of cardiac mitochondrial function, such as ATPase reaction, and alterations in the cardiac mitochondrial calcium translocation.[59]

As stated earier, adriamycin, daunomycin, and other anthracycline antibiotics stimulate the formation of superoxide anion radical, hydrogen peroxide, and hydroxyl radical by subcellular fractions.[60] The major site of these reactive components formed in the heart is at the Complex I of the mitochondrial electron transport chain.[61] The heart has been shown to have a decreased capacity to detoxify these reactive species. This in turn makes it susceptible to anthracycline induced oxygen radical damage. The heart has limited amounts of superoxide dismutase, catalase, and glutathione peroxidase which are used by other tissues to eliminate reactive oxygen species.

Lipid peroxidation, a free radical mediated event,[62] has also been proposed as a possible biochemical mechanism of cardiotoxicity, both in vivo and in vitro. Several studies have indicated that anthracycline-mediated lipid peroxidation occurs only in the presence of trace amounts of iron.[63] Other studies indicate a mechanism in which direct reaction with iron could stimulate lipid peroxidation without the need of redox cycling of the anthracycline

compound.[64] This involves the drug molecule forming very strong complexes with iron causing the complex or chelation to increase the electrophilic character of the drug.

The effect of daunomycin and adriamycin and their complexation to Fe(III) was studied to determine the effect of lipid peroxidation in intact human platelets. Adriamycin and daunomycin and Fe(III) quickly induced lipid peroxidation as measured by the thiobarbituric acid assay.[65] In an attempt to develop a method to define the role of free radicals and lipid peroxidation in the cytotoxicity of adriamycin, adriamycin-induced lipid peroxidation was measured by the formation of malondialdehyde (MDA) formation in the rat globlastoma cells. Adriamycin-induced lipid peroxidation was maximal 24 hours after incubation of cells with the drug. This indicated that a lag time was necessary for the free radical-mediated membrane damage induced by adriamycin, to occur. In the presence of alpha-tocopherol in the culture medium, the drug-induced MDA formation was inhibited.[66] Lin et al.'s[67] study on the effect of schisanhenol (Sal) on adriamycin-induced heart mitochondrial toxicity concluded that there were no changes in cytotoxicity, but a decreased amount of carditoxicity was observed.

D. Second Generation Anthracyclines

The cardiotoxicity of daunomycin and adriamycin has provided the main rationale for the extensive isolation and synthetic programs for second generation anthracycline analogs/derivatives. Although there have been many

anthracyline derivatives synthesized and characterized,[68] 5-iminodaunomycin (a C-5 derivative of daunomycin) displayed in Figure 6 was the first quinone-modified analog of daunomycin and adriamycin with promising non-cardiotoxic success.[69] It has been the focus of extensive investigation because of its diminished cardiotoxicity activity while retaining cytotoxic properties. It been successful as a potent agent that is used to treat P-388 leukemia.[70] It has shown to be 10-fold less cardiotoxic than adriamycin in isolated rat myocytes.[71] To produce the the same degree of cardiotoxicity, 5-iminodaunomycin would have to be administered 4.5-fold times compared to daunomycin.[72] The diminished cardiotoxicity has been associated with the decreased capacity to undergo catalytic production of reactive oxygen species which has been shown to occur with daunomycin and adriamycin.[73] In-vitro studies showed signs that there were alterations in the DNA interactive properties that may be responsible for its mode of action.[74] The analog showed complete loss of mutagenicity to Salmonella typhimurium in a Ames test.[75] In the same instance, both daunomycin and adriamycin show opposite effect (mutagenicity was observed). Cytokinetic and biochemical effects of the derivative was compared to adriamycin to examine if modification of the benzoquinone moiety to produce low levels of radical productions would alter RNA and DNA processes. It was established that RNA synthesis was not inhibited after administration of the analog. However, after the administration of adriamycin, both RNA and DNA synthesis was impaired. This could possibly have

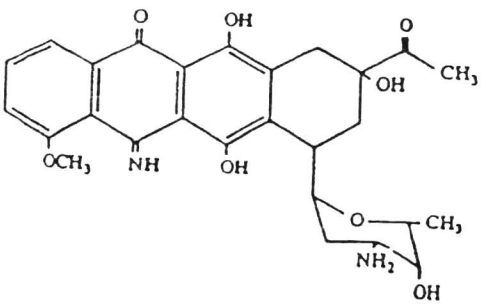

5-iminodaunmycin

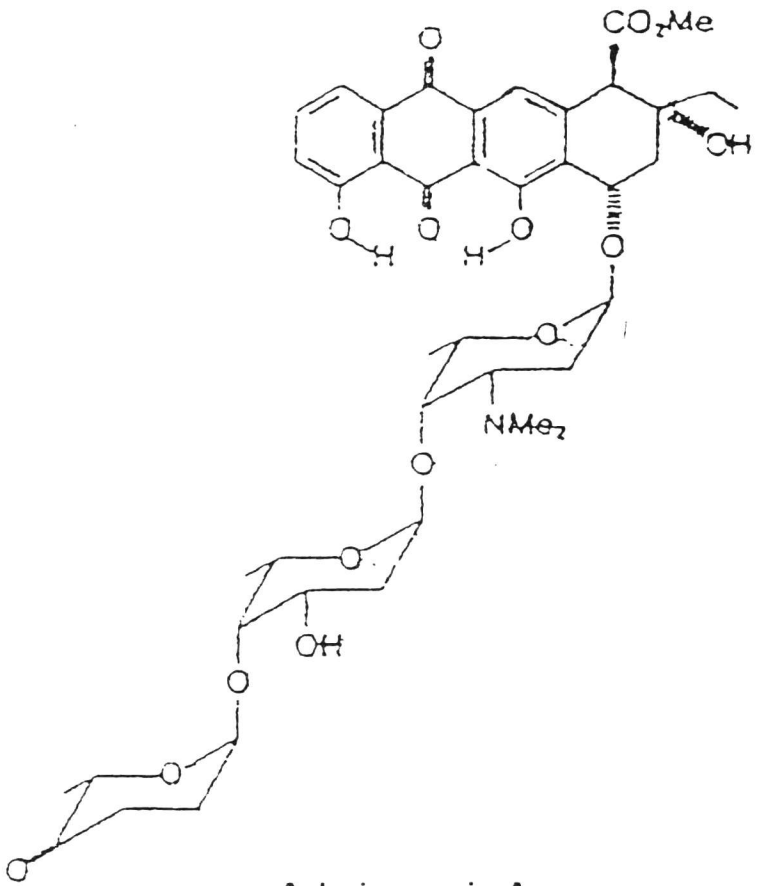

Aclacinomycin A

Figure 6. Structures of 5-iminodaunomycin and aclacinomycin A.

implication for the differences in cardiotoxicity.[76]

Since the demonstration of outstanding safety of 5-iminodaunomycin, other anthracyclines reported to have less cardiotoxicity than adriamycin and daunomycin include: 4'-epidoxorubicin, 4'-deoxydoxorubicin, 4'demethoxydaunorubicin, 4-demethyldaunomycin, aclacinomycin A, menogaril, AD-32, and MRA-CN.[77] To date, daunomycin and adriamycin have demonstrated high efficacy, but because of cardiotoxicity, usage of these drugs have greatly limited their adminstration. Because of this undesirable side effect, these and other anthracycline drugs have continued to undergo intensive chemical, biochemical, physical, and structure-activity relationship studies.

These first generation anthracyclines (i.e. adriamycin and daunomycin) are the first agents of the drug class to be isolated from Streptomyces and found to be therapeutically active. They are complex anthraquinone systems proposed to undergo redox-cycling forming reactive radical systems. These redox states/intermediates have been implicated to transfer electrons to molecular oxygen forming superoxide, hydrogen peroxide, and hydroxyl radicals.[37] These oxygen species have been implicated to be responsible for (or partially responsible for) cardiotoxicity, the dose-dependent side effect which have greatly limited anthracycline adminstration.

5-iminodaunomycin, a second generation anthracycline (isolated from mutant strains of Streptomyces), has displayed remarkable reduced cardiotoxicity while retaining aprreciable cytotoxicity, compared to its first

generation counterpart (daunomycin). This has been proposed to be because of its diminished capacity to produce the highly reactive oxygen species which occur with the first generation drugs.

The activation/reduction of anthracyclines (anthraquinone systems) have been proposed to proceed via two electron/two proton attachments.[79] One mode of this activation can be visualized using 1,4-benzoquinone (a simple quinone) as a model (displayed in Figure 7). Reductive activation of the benzoquinone (and anthraquinone) system as shown in the Figure proceed through the following redox states (in the order of): quinone (Q), quinone radical anion ($Q^{-\cdot}$), semiquinone radical ($QH^{\cdot}$), semiquinone anion (QH^{-}), and hydroquinone (QH_2), the final reduction state of the activation.

To date, a thorough understanding of how the intermediates, $Q^{-\cdot}$, $QH^{\cdot}$, QH^{-}, and QH_2 participate in the anthracycline's cardiotoxicity dilemma has been lacking because they are highly energetic and have short lifetimes. Thus, the understanding how these species contribute to overall biochemical activity are of crucial importance.

Since these highly reactive systems (radicals) are not readily amenable for experimental investigation, redox states of some substituted and unsubstituted benzoquinone/naphthaquinone systems (in addition to their isoelectronic imine and diimine analogs) were subjected to a AM1 semiempirical molecular orbital study.

The aim of this study, was to use the theoretical approach to determine

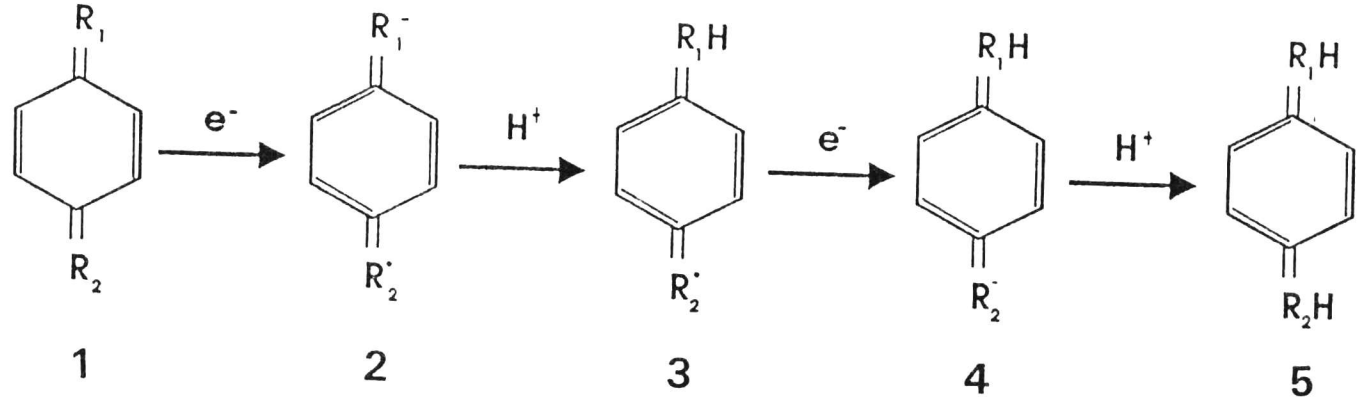

Figure 7. A possible reduction mechanism for quinones. 1,4-Benzoquinone where R_1 and R_2 is O; imine-benzoquinone where R_1 is O and R_2 is NH, and diimine-benzoquinone where R_1 and R_2 are NH.

the relative reactivity of each quinone redox state and to correlate their electronic properties with biological activity. This approach uses pre-determined experimental parameters and valence electron molecular orbital components to compute the optimized electronic properties (the wavefunction) of a molecule. Systems investigated in this study are located in Figure 8. The systems displayed are 1,4-benzoquinone (I), 1,4-naphthaquinone (II), hydroxy-naphthaquinone (III), 5,8-dihydroxy-1,4-naphthaquinone (IV), and 5,8-dihydroxy-iminenaphthaquinone (V). In addition to the systems listed, imine- and diimine- analogs of 1,4-benzoquinone and the imine- analog of dihydro-1,4-naphthaquinone were also investigated in comparison to their parent counterpart. As mentioned earlier, 5-iminodaunmycin has demonstrated reduced cardiotoxic activity. All systems were studied because each moiety can be found in one of the anthracycline drugs (except the diimine systems). The diimine system was studied because of reduced toxicity observed for 5-iminodaunomycin. It may be that this moiety, if part of the overall drug system, may present better cytotoxic and cardiotoxic results than its imine analog. These systems (all with quinone, imine-quinone, or diimine-quinone character) were also studied in an attempt to better understand their overall participation and role in the anthracycline drug class reactivity.

The model systems (I-V, Figure 8) chosen in this study are all part of the pharmacophore of the anthracyclines. Specifically, I is a part of a good number

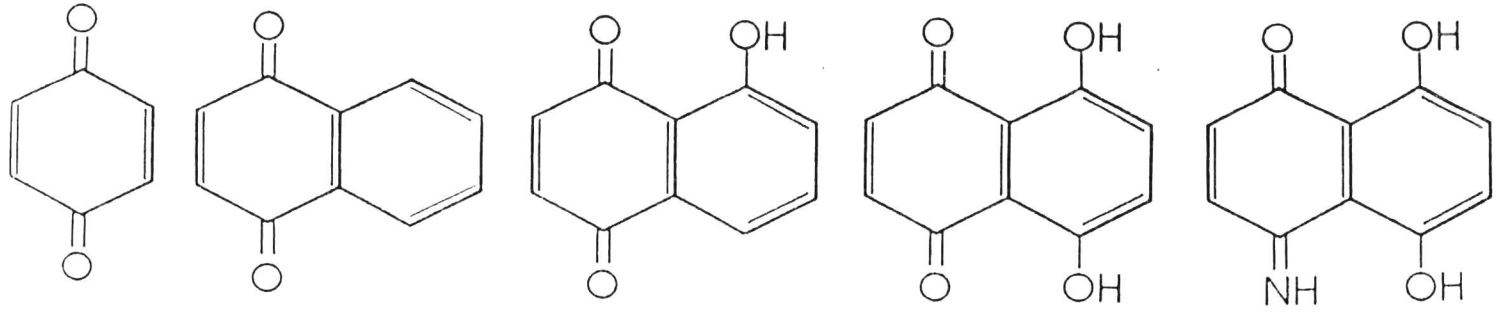

I II III IV V

Figure 8. Some quinone systems investigated in this study.

of anthracyclines and has been speculated to be the portion of the drug system that leads to the reductively activated species which are speculated to participate in undersirable electron-transfer reactions; II, substituted, has been indicated to have antitumor activity against Ascitic Sarcoma 180 in mice;[80] III, part of the aclacinomycin A molecular makeup, has demonstrated reduced cardiotoxic activity compared to adriamycin and daunomycin; System IV, a major part of both adriamycin and daunmycin, is speculated to produce highly reactive species; and lastly, system V, which is part of the molecular structure of 5-iminodaunomycin has also demonstrated reduced carditoxicity relative to its parent analog, daunomycin.

Within the validity of Koopman's theorem,[81] parameters used in this comparative study were absolute electronegativity, absolotue hardness, and reaction enthalpies. All values (with the exception of reaction enthalpies) were computed from the AM1 molecular orbital energies. Reaction enthalpies were calculated from the AM1 heats of formation values.

Parameters obtained in this study were also subjected to a least squares linear regression approach using the Sigma plot program.[82] Groups[83,84] which had investigated the relationship between frontier molecular orbital parameters and reduction potential had concluded that the HOMO-LUMO gap (η) correlated well with experimental values. It was thus of interest to see if various results from this study could be correlated with reduction potential which in turn have been shown to correlate with biological activity.[84] The five calculated

parameters used for the correlation study were χ, η, ΔH_f, SOMO and LUMO energies. To our knowledge, a simultaneous determination of these five parameters and their correlation with experimental reduction potential have not been performed. From the point of view of correlating electronic properties with biological activity, using more parameters may give additional and/or new information on the overall reactivity of highly reactive species.

From the regression analysis, correlation coefficients data were extracted from each regression analysis and used to determine the goodness of the fit. Correlation coefficients obtained for the SOMO and LUMO energies, reaction enthalpies for electron attachment, chemical hardness, and electronegativity values showed reasonably good correlations which indicates that this study may have some relevance in determining parameters for systems not readily available for experimental investigation (i.e. radical systems).

This theoretical approach has been used to investigate simple quinone systems to model the anthracycline class of drugs. Parameters determined from the analysis were used to assess the relative reactivities and stabilities of the reductively-activated intermediates in an attempt to gain insight into the various electron transfer reactions which are speculated to be responsible for the cardiotoxic effects of the drugs. This initial study was conducted with the hope to ultimately correlate electronic properties of each intermediate in the quinone reduction process (especially the radical species) to biological activity.

II. THEORETICAL APPROACH

Currently there are four theoretical procedures available for the study of properties of molecules. They are ab initio, semiempirical molecular orbital methods, density function methods, and molecular mechanics. All methods, with the exception of molecular mechanics, are quantum mechanical techniques which can be utilized to investigate correlations between electronic structure and biological activity. The theoretical approach taken in this study was the semiempirical molecular orbital method using the AM1 formalism.[85]

The semiempirical molecular orbital methodology, for this investigation, is the method of choice for large systems because it determines optimized electronic parameters based on outer (valence) electrons for complex organic molecules. The method simplifies quantum mechanical calculations on systems of chemical interest unlike ab inition methods where all electrons in the molecule are included and determination of optimized parameters may be difficult or impossible due to the size of complex molecules and/or computation time of the method. Accuracy of some semiempirical methods have approached data similar to ab initio STO-3G methods.[86]

Recent concepts from hard-soft acid-base and density functional theories[87] allow the calculations of electronegativity, chemical hardness, and other molecular parameters that can be used to describe chemical reactivity in electron transfer reactions.[88] For this study, it is of importance to investigate the elctronic properties of benzoquinone (I), para-benzoquinone imine (VI), and

para-benzoquinone diimine (XI) to establish correlations between electronic and biological activities.

A. THEORY

The AM1 semiempirical method employs the theory of effective valence shell Hamiltonian.[89] The method combines calculations of vibrational spectra, thermodynamic quanties, isotropic substitution effects, and force constants to computed results. It is a all self-consistent (SCF) procedures that take into consideration, electronic repulsion and exchange stabilization using calculated integrals which are determined by approximate means. Additionally, it uses restricted basis set of one s orbital and three p orbitals per atom and neglect the overlap integrals in the secular equation. The original equation is modified from:

$$|H-ES| = 0 \qquad (1)$$

to the modified expression:

$$|H-E| = 0 \qquad (2)$$

where H is the secular deteminant, S is the overlap matrix and E is the set of eigenvalues.[90] AM1 uses single-atom parameters to calulate two-electron one-center integral from atomic spectra. AM1 combines experimental calculations of vibrational spectra, thermodynamic quantities, isotropic substitution effects, and force constants to compute parameters.

A spectrum of molecular orbital approximations are given in Table 1. The ab initio method is the most accurate while the Huckel method is the least

Table 1. Spectrum of wavefunctions

The Least Accurate,	➢ Simple Hückel
Fast and Cheap	➢ Free Electron
	➢ Extended Hückel
	➢ Pariser-Parr-Pople
	➢ CNDO
	➢ INDO
	➢ MINDO
	➢ MNDO
	➢ AM1
	➢ PM3
The Most Accurate,	➢ PRDDO
Slow and Expensive	➢ Ab Initio

accurate. AM1, the approximation used in this investigation, was developed as a result of errors in MNDO.[85] MNDO approximations had a tendency to overestimate repulsion between atoms in a molecule. This overestimation was most likely a result of the core repulsion function (CRF). Therefore, the formalism used in AM1 is essentially the same as in MNDO with the exception of the CRF.

B. METHOD

Structures, energies, and energetic properties of all systems were calculated using restricted and unrestricted Hartree-Fock AM1 formalism. Force constants were used to verify that the equilibrium geometries were potential energy minima.

The programs used in this AM1 theoretical study were AMPAC[91] and MOPAC,[92] obtained from Quantum Chemistry Program Exchange (QCPE). Prior to MOPAC calculations, initial input planar structures were generated and optimized using PCMODEL[93] on a HP Personal Computer. All other calculations were performed on the VAX 8550 system. Keywords[94] used in calculations were GRADIENTS, LOCAL, ENPART, PRECISE, POWELL, BONDS, VECTORS. Parameters generated from the program were obtained utilizing the Broyden-Fletcher-Goldfab-Shanno optimization procedure with respect to all structural variables. Molecular geometries were calculated by minimizing the total energy with respect to all geometrical parameters using keywords listed above. They were optimized without assuming any restraints. All frontier molecular orbital

energies were extracted for optimized structures and used to calculate chemical potential, electronegativity, and chemical hardness within the validity of Koopman's theorem.[81]

Reaction enthalpies were calculated for various electron and proton attachments which are feasible for benzoquinone and its analogs. Values calculated should give indication to the overall reactivity of an activated system. Heat of formation values were extracted for the activated forms and used to calculate the reaction enthalpy (ΔH_{rxn}):

$$\Delta H_{rxn} = \Delta H_f f\ (P) - \Delta H_f\ (R) \quad (3)$$

where P and R denote products and reactants, respectively (for examples for $Q + e^- \text{---} > Q^{\cdot -}$, where Q is the reactant and $Q^{\cdot -}$ is the product).

Chemical potential (μ) was calculated using the following equation: $\mu = -(I + A)/2$ where I is the ionization potential (negative of the highest occupied molecular orbital, (HOMO) energy)) and A is the electron affinity (negative of the lowest unoccupied molecular orbital, (LUMO) energy)). Chemical potential is a property that measures the escaping tendency of electrons in a species.[95] It's constant throughout the molecule. For radical systems, I is taken to be the negative of the singly occupied molecular orbital (the SOMO) energy. The higher the chemical potential, the greater tendency it has to transfer electrons. Electronegativity (χ) is equal to the negative of the chemical potential energy. Electronegativity is defined as the ability of an atom to attract electrons within a molecule to itself. Both parameters (chemical potential and electronegativity)

determine the extent by which the chemical species is able to transfer its electron to other chemical species.[96] Both μ and χ are molecular properties and not orbital proteries and each value are found to be constant throughout the entire molecule.

Absolute hardness (η),[97] is the HOMO-LUMO gap. It's the resistance of the chemical potential or the sensitivity of the electronegativity [98] to change in the number of electrons. The operational definition of hardness is: $\eta = (I-A)/2$, where I and A are defined above. Hardness (companion to absolute electronegativity)[87] determines the magnitude of total electron transfer. Hardness, unlike μ and χ, varies from from atom to atom within a molecule. Recent studies have correlated biological activity with redox potential.[99] Also, correlations of redox potential and the HOMO-LUMO gap (hardness) has been demonstrated. Knowing this, the molecular parameter, η, was examined closely in this investigation to establish correlations between the reactivity of activated species and biological implications. Correlations of redox potential with SOMO energies, LUMO energies, and heats of formation were also investigated. All correlation values were extracted using the Sigma Plot program (version 4.0)[82] from a linear regression analysis.

III. RESULTS AND DISCUSSION

Model systems investigated in this study are displayed in Figure 8. One mode of their reductive activation is shown by the proposed mechanism in Figure 7. Through two electron and two proton attachments, the quinone system (including derivatives) may be reduced to its hydroquinone state according to the following equation:

$$Q + 2e^- + 2H^+ \text{--------}> QH_2 \qquad (4)$$

Species 1, 2, 3, 4, and 5 depicted in Figure 7 are the quinone, quinone radical anion, semiquinone, semiquinone anion and hydroquinone states, respectively, of I, VI, XI. In upcoming sections, a comparative treatment of similar ring systems (one- and two-ring) will be evaluated separately utilizing the different theoretical parameters identified in Section II.

A. COMPARISON OF ONE-RING SYSTEMS

Geometrical Reorganization: Comparison of 1,4-Benzoquinone (I) and its Analogs Para-Benzoquinone Imine (VI) and Para-Benzoquinone Diimine (XI). These systems are displayed in Figure 9. The reduction activation of the quinone moieties of the anthracycline drugs should induce considerable reorganization in electronic structure which should in turn be manifested as changes in geometry, electron affinity, electronegativity (or electronic chemical potential), and absolute hardness. The reorganization in the electronic

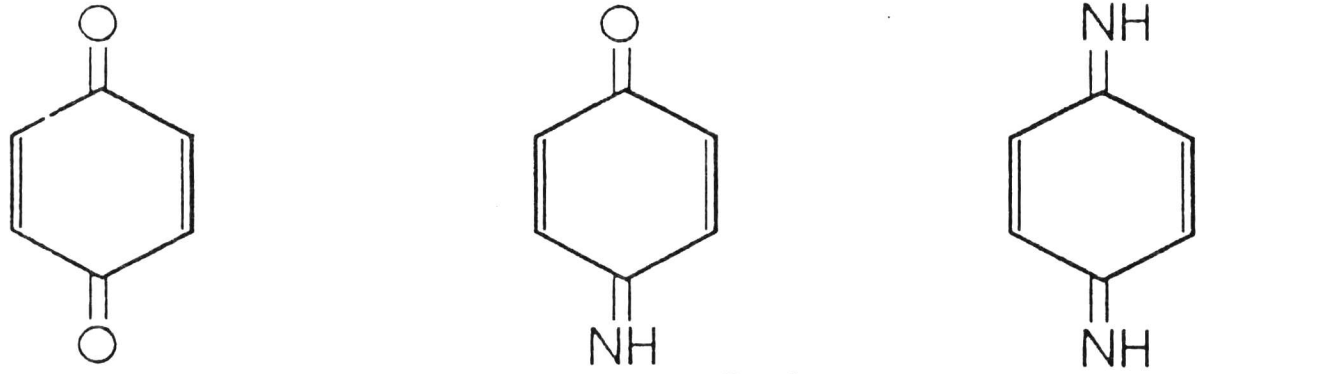

I. VI. XI.

Figure 9. Structures of benzoquinone (I), and its imino- (VI), and diimino- (XI) analogs.

structures of I, VI, and XI as they undergo the reactions in the scheme displayed in Figure 7 can be assessed by analyzing bond lengths and bond and torsional angles. Considering just a few of the steps in Figure 7, for example, comparison of these geometric parameters for I-III, VI-VIII, and XI-XIII revealed several features (with trends that were very similar in going from I-->II-->III, from VI ---> VII ---> VIII and to a larger extent from XI ---> XII ---> XIII (Figure 10)): some bond lengths increased with concomitant decrease in others indicating extensive p-electron delocalization over molecular fragment such as $O_2(N_2)$-C_1-C_3-C_5-C_7-$C_8(N_8)$ (Figure 11); protonation increased some bond lengths while it decreased others; most localized bonds were C_1-O_2 and C_1-N_2; salient changes in bond angles were observed with no clear trend; most torsional angles were found to be 0° or 180° indicating planarity; VIII and XIII were not planar since the torsional angles were very different from 0° or 180°. The non-polar geometries for VIII and XIII suggest the hybridization must have changed considerably.

Table 2 shows selected energetic properties and a dissection of the total energies, E_t into one- and two-center terms. The energy partitioning analysis[100] can be used to determine the origin for the favorability and/or unfavorability of a given reaction over any other in Figure 7. For example, the reaction enthalpies and the total energies show that formations of II from I, and of VIII form VII are more favorable over that of VII from VI, and III from II respectively. The partitioning analysis showed that the reason formation of II from I is

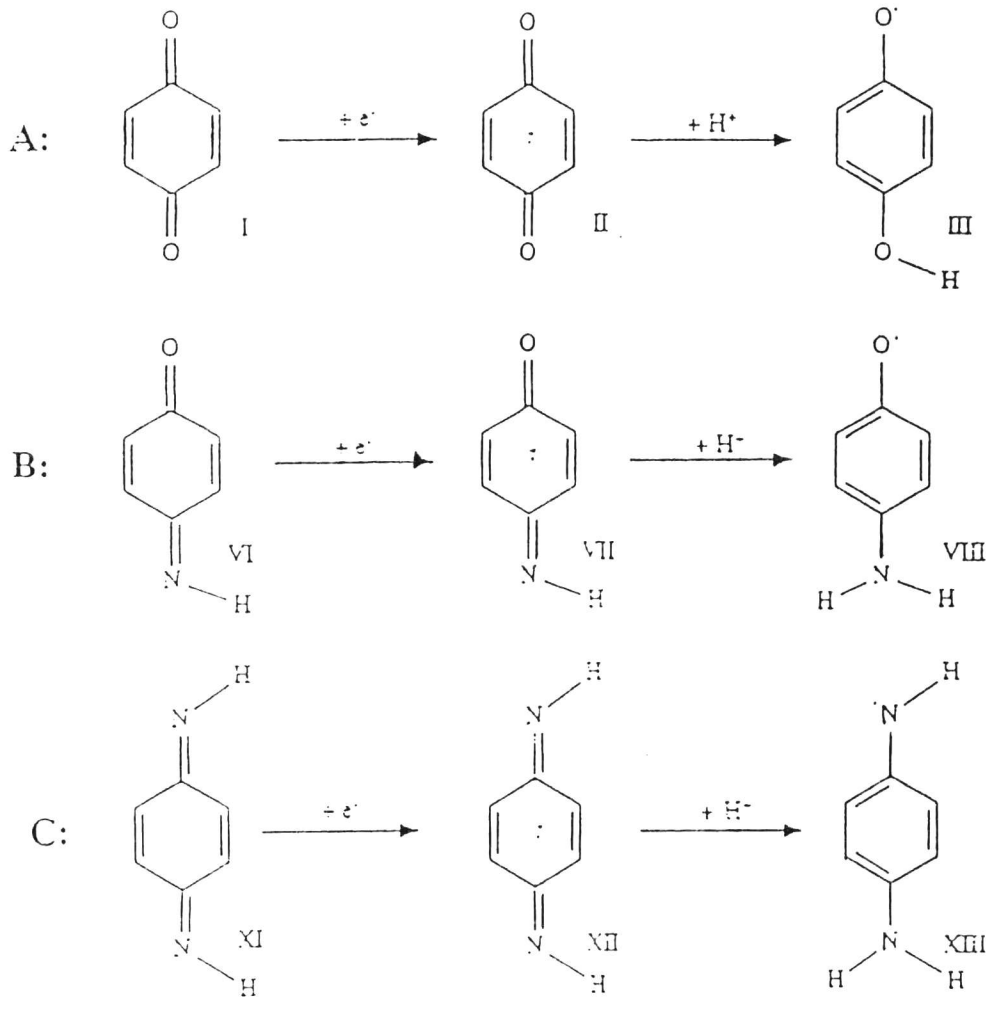

Figure 10. Reduction of benzoquinone and its analogs through one electron and one proton attachments.

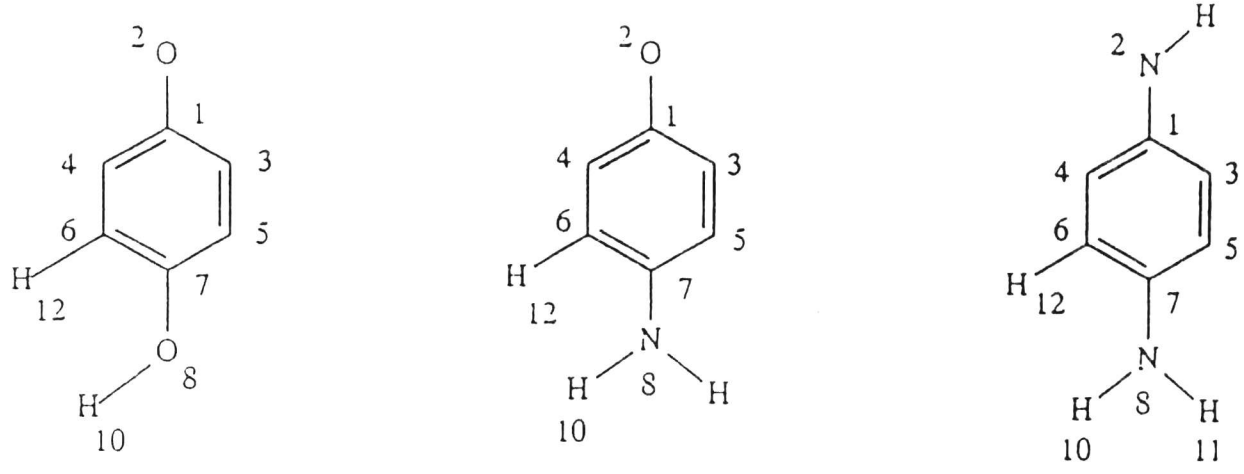

Figure 11. Numbering scheme for the semiquinone anion of benzoquinone (IV), and its imine- (IX), and diimine-(XIV) analogs.

TABLE 2. Selected energetic properties for I-III, VI-VIII, and XI-XI as calculated with AM1.

	ENERGY								
PARAMETER	I	II	III	VI	VII	VIII	XI	XII	XIII
ΔH_f	-25.08	-76.93	-41.49	23.62	-22.93	-0.55	73.5	33.36	46.19
ΔH_{rxn} (1)		-51.85	-16.41		-46.55	-24.17		-40.14	-27.31
ΔH_{rxn} (2)			35.44			22.38			12.83
E_1 (eV)	-1261	-1266	-1271	-1149	-1155	-1156	-1038	-1044	-1047
E_2 (eV)	-207.9	-206.1	-211.2	-220.0	-121.0	-228.6	-231.8	-228.1	-238.3
E_3 (eV)	-6.72	7.72	6.32	6.98	7.83	7.76	7.09	7.70	7.68
E_t (eV)	-1462	-1465	-1477	-1363	-1365	-1377	-1263	-1264	-1278
IP	10.88	2.77	9.14	10.46	2.59	8.49	9.77	2.41	8.33
D	0	0	3.276	2.319	2.071	5.009	2.54	1.89	3.34

$\Delta H_{(1)}$ presents: ΔH_f of II and III minus that of I; ΔH_f of VII and VIII minus that of VI; ΔH_f of XII and XIII minus that of XII. $\Delta H(2)$ represents: $\Delta H_{f,III} - \Delta H_{f,II}$; $\Delta H_{f,VIII} - \Delta H_{f,VII}$ and $\Delta H_{f,XIII} - \Delta H_{f,XII}$; E_1 = sum of one-center terms, E_2 = sum for two-center neighboring pairs, E_3 = sum of two-center nonneighboring pairs; $E_t = E_1 + E_2 + E_3$; IP = ionization potential (eV); D = dipole moment (Debyes). ΔH_f is the heat of formation computed from AM1.

favored over that of VII from IV, albeit in the gas phase, is the result of the destabilizing effect of the two center neighboring or bonding pair interactions. A similar analysis can be made for the protonation process. The energy partitioning analysis for the protonation process also showed that the reason why formation of VIII from VII is more favorable over that of III from II is a result of the stabilizing energy contribution due to again the two-center neighboring pair interactions. The partitioning of the total energy seems to indicate that the favorability of electron and proton attachments in I, VI and XI is governed by the two-center neighboring pair interactions, i.e., interactions between atoms within 1.9°A of each other. The data given in Table 2 partially reflected the reorganization of the electronic structures of quinone and its analogs as they undergo reduction. Further insight into these structural changes can be gotten from quantification of interatomic interactions[101] via the energy partitioning analysis technique.[100] Figures 12-13 shows some selected pair interactions from which an assessment of stabilizing (negative values) and destabilizing (positive values) effects can be determined. For bonding pair interactions the magnitude of the energy, which is due to the contribution of the one-electron core resonance integrals to the energy of a bond, reflects the strength of the bond between the atoms of the pair. It is evident from the data in the Figure how the pair interactions change for the first two steps of Figure 7. What is of interest is of course how these changes manifest themselves in the reactivity of the species resulting from the reduction.

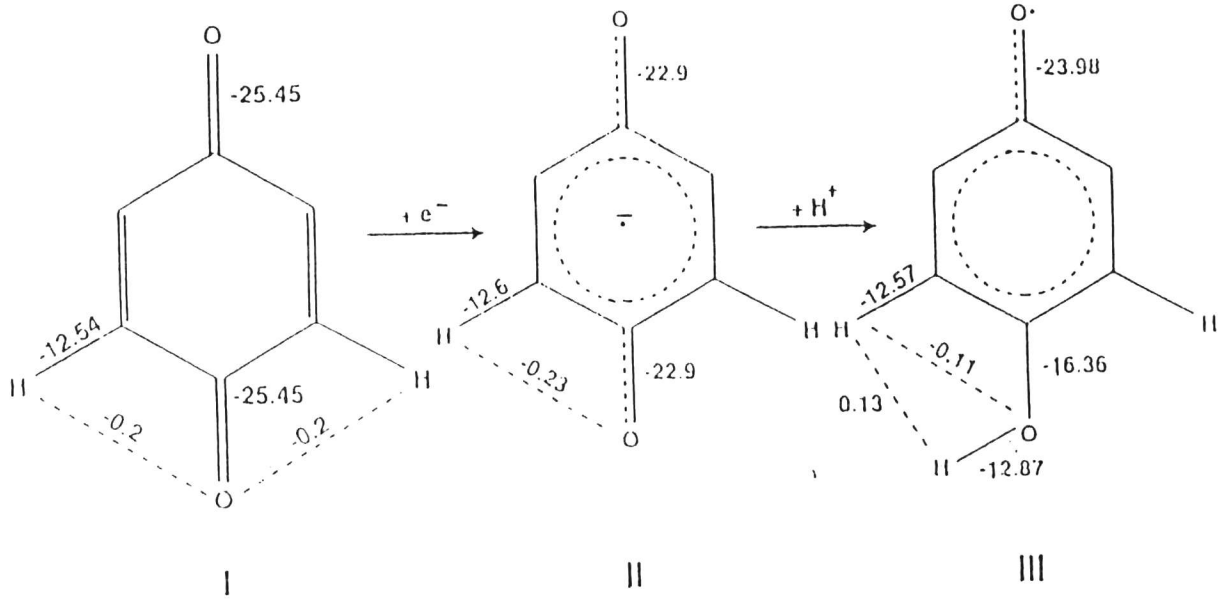

Figure 12. Selected pair interactions of stabilizing and destabilizing effects of structures I-->III.

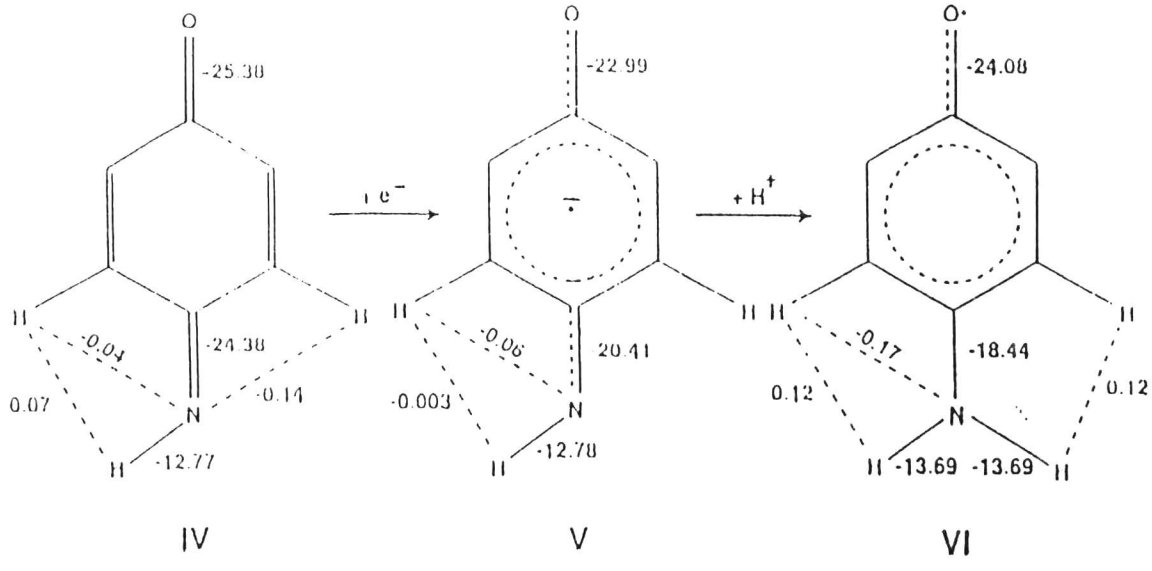

Figure 13. Selected pair interactions of stabilizing and destabilizing effects of structures IV--> VI.

Relative Importance of Electron and Proton Attachments. The calculated reaction enthalpies for the various electron and proton attachment steps according to Figure 7 and their combinations are summarized in Table 3. The Table also provides the decreasing order in ease of electron or proton attachment for the various steps or combinations thereof in Figure 7. Several conclusions can be made from the data: (1) replacement of O by NH: (a) makes electron attachment less favorable, (b) makes proton attachments more favorable, (c) the order for ease of electron attachment is the reverse of that of proton attachment; (2) the trends for semiquinone and hydroquinone formations follow that of proton attachment; (3) the trend for electron attachment to the semiquinone ($QH^{\cdot}$) (3-->4) giving the semiquinone anion (QH^{-}) is different from the overall trend for QH^{-} formation (1-->4); (4) the trend for the overall hydroquinone (QH_2) formation $QH^{\cdot}$ (3-->5); (5) since the trends for $QH^{\cdot}$ and QH_2 formation (1-->3 and 1-->5, respectively) follow the trend for proton attachment, proton attachment seems to govern the enthalpy of $QH^{\cdot}$ and QH_2 formation; (6) the overall QH^{-} formation (1-->4) and QH_2 formation from $QH^{\cdot}$ (3-->5) are different from the patterns for electron and proton attachments.

The data overall show the relative importance of the electron and proton attachment steps in reductive activation of quinone and its isoelectronic derivatives. It is interesting to note that the overall semiquinone anion (QH^{-}) formation is favored in VI. The thermodynamic calculations also suggest that

Table 3. **AM1 calculated reaction enthalpies (ΔH_{rxn})[a] for electron and proton attachments in one-ring systems (pertaining to the scheme in Figure 7)[a].**

Process	I	VI	XI	ORDER
Electron Attachment				
1------>2	-51.85	-46.56	-40.14	I>VI>XI
3------>4	-45.14	-40.75	-27.62	I>VI>XI
Proton Attachment				
2------>3	35.44	22.29	12.83	XI>VI>I
4------>5	20.91	18.45	1.23	XI>VI>I
Semiquinone Formation				
1------>3	-16.41	-24.27	-27.31	XI>VI>I
Semiquinone Anion Form.				
1------>4	-61.55	-65.01	-54.94	VI>I>XI
Hydroquinone Formation				
1------>5	-40.63	-46.57	-53.70	XI>VI>I
3------>5	-24.23	-22.30	-27.31	XI>I>VI

[a] Values are given in kcal/mol.

if $Q^{\cdot-}$ is primarily responsible for toxicity, substitution with N should lead to reduction in toxicity because less of the reduced species should form in the N-substituted case. But if $Q^{\cdot-}$ is readily protonated, to $QH^{\cdot}$ for example as expected since protonation is diffusion controlled, and if $QH^{\cdot}$ and/or QH_2 are responsible for toxicity, the thermodynamic consideration suggests that substitution with N should lead to more toxicity. The calculations of course did not incorporate medium effects due to such as hydration environments and do not allow one to reach definitive conclusions. They are however instructive and give come insight into the rational design of imino- and amido-derivatives of quinone- and anthraquinone containing drugs.

Possible reductive routes for the conversion of VI to the hydroquinone form (X) are displayed in Figure 14. The route in Figure 7 is denoted by route A1 in Figure 14 and it is evident from the overall reactions enthalpies that routes A1 and B1 are equally favorable (Figure 14), although individually corresponding steps in the two routes are not. Route B1 is therefore a viable route in the reduction of VI to X. On the other hand, routes A2, A3 and B2 probably do not contribute to the overall reductive process as can be judged from the calculated reaction enthalpies for these routes. Conversion of the semiquinones ($QH^{\cdot}$) of I and XI can also take place via routes shown in Figure 15, but these routes are not as favorable as the routes in Figure 7. In any case, since the cationic radicals 7, 8, 9 and 10 (Figures 14 and 15) are electron-deficient, they are not expected to transfer electrons to other species

and are not considered further in this work, except to mention that if they do form, they can act as oxidizing agents.

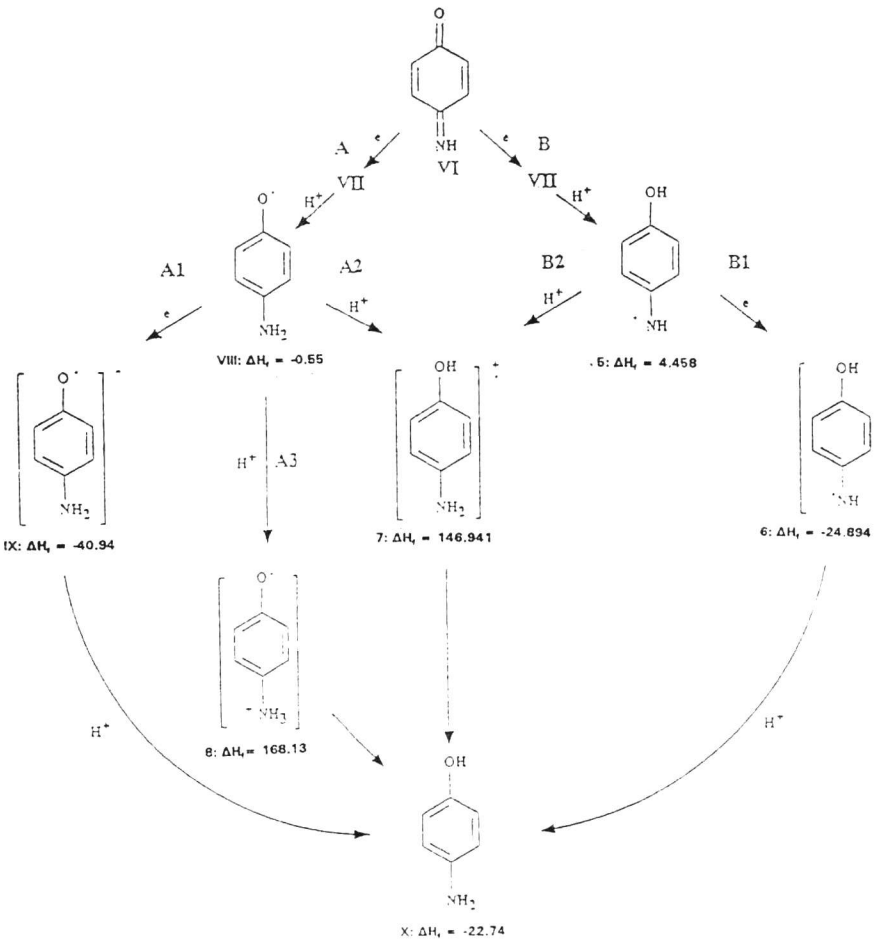

Figure 14. Possible reductive route for the conversion of VI to X. ΔH_f's for VI and VII are located in Table 2.

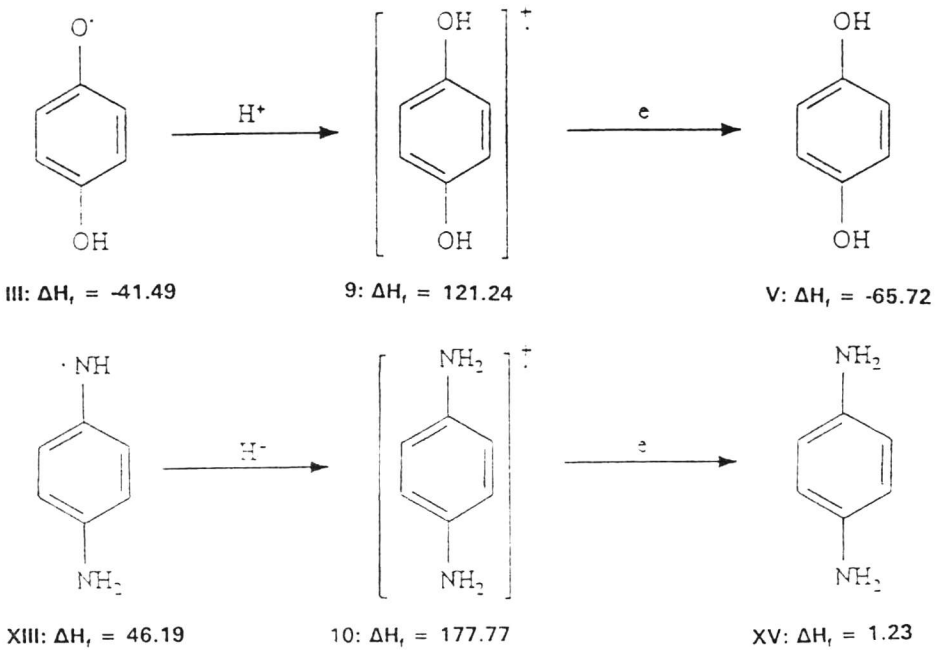

Figure 15. Alternative routes for the conversion of the semiquinones I and XI to V and XV, respectively.

Topology-Micromechanism Considerations in Reductively-Activated I, IV and VII. Another example of changes in molecular structure organization is illustrated in Figure 16-18. In the Figures, the intermediate geometries of I and the respective analogs from VI (and XI) are compared. Figure 16 shows pluto drawings of the geometries of III and VIII. The geometries obtained for the anions from III and VIII are presented in Fig 17. The salient differences between the geometries of III and VIII can be determined by visual examination. Electron attachments to III and VIII can lead to rotamers devoid of planarity as can be seen in Figure 17. Based on calculated heats of formation, the geometries of the rotamers in Figure 17, (i.e., IV and IX) are actually more favored over their planar counterparts by 1.2 and 6.69 kcal/mol.

In light of one of the attributed modes of action of the anthracyclines, which is the intercalation of the anthraquinone moiety of the drugs between DNA base pairs, this is a most interesting result. The geometries in Fig. 17 strongly suggest that complete intercalation probably does not take place with such geometries. If the semiquinone anions of the drug can form once the drug is administered to a patient, the geometrical constraints would probably prohibit at least one side of the anthraquinone portion of the drug molecule from intercalating between the DNA base pairs and a mechanism that does not include intercalation may be invoked. These reactive species may, therefore, react with biological molecules only in a nonspecific way at a site where they are produced. Philips and Crothers[102] have reported a

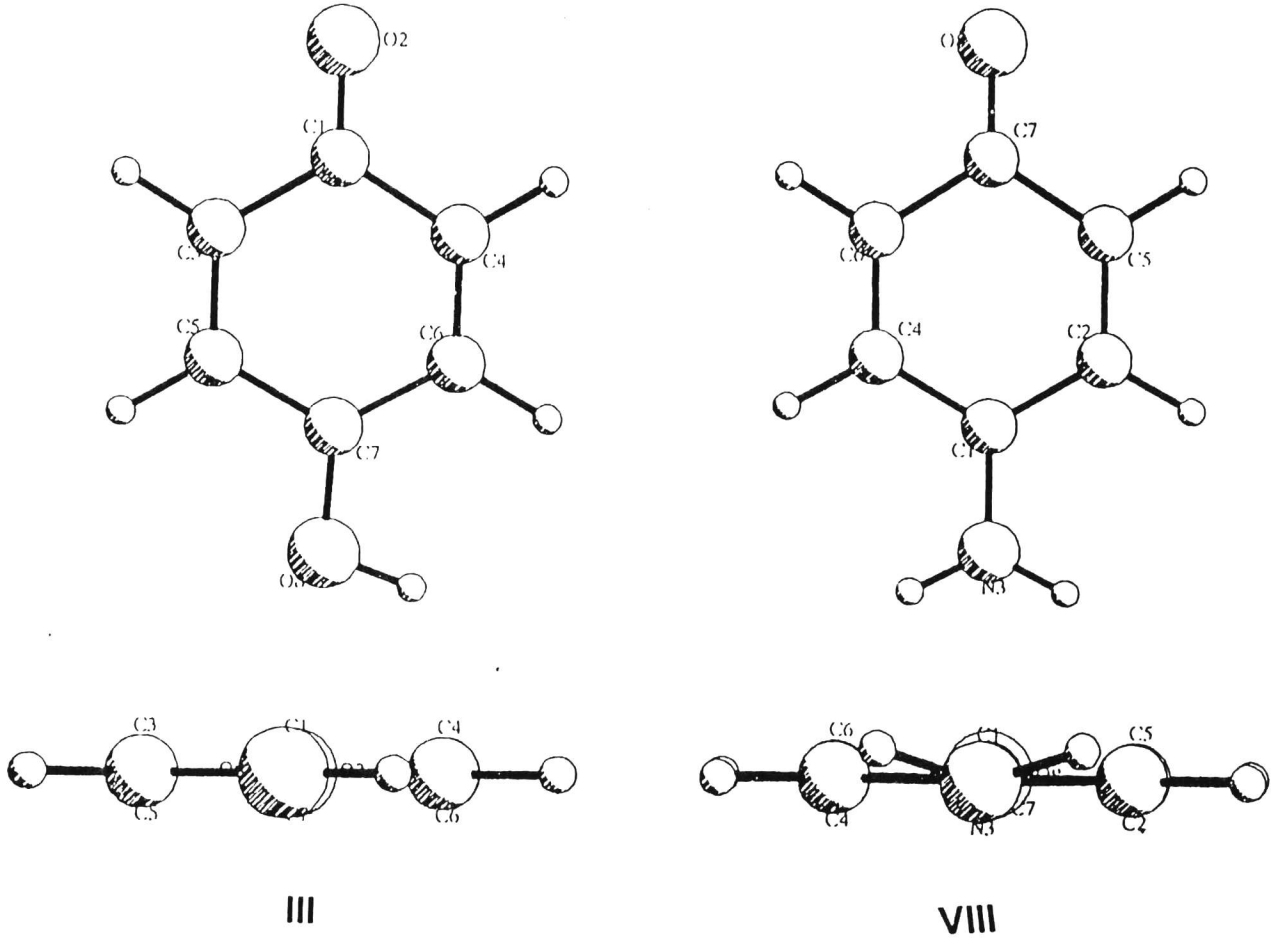

Figure 16. Pluto drawings of III and VIII.

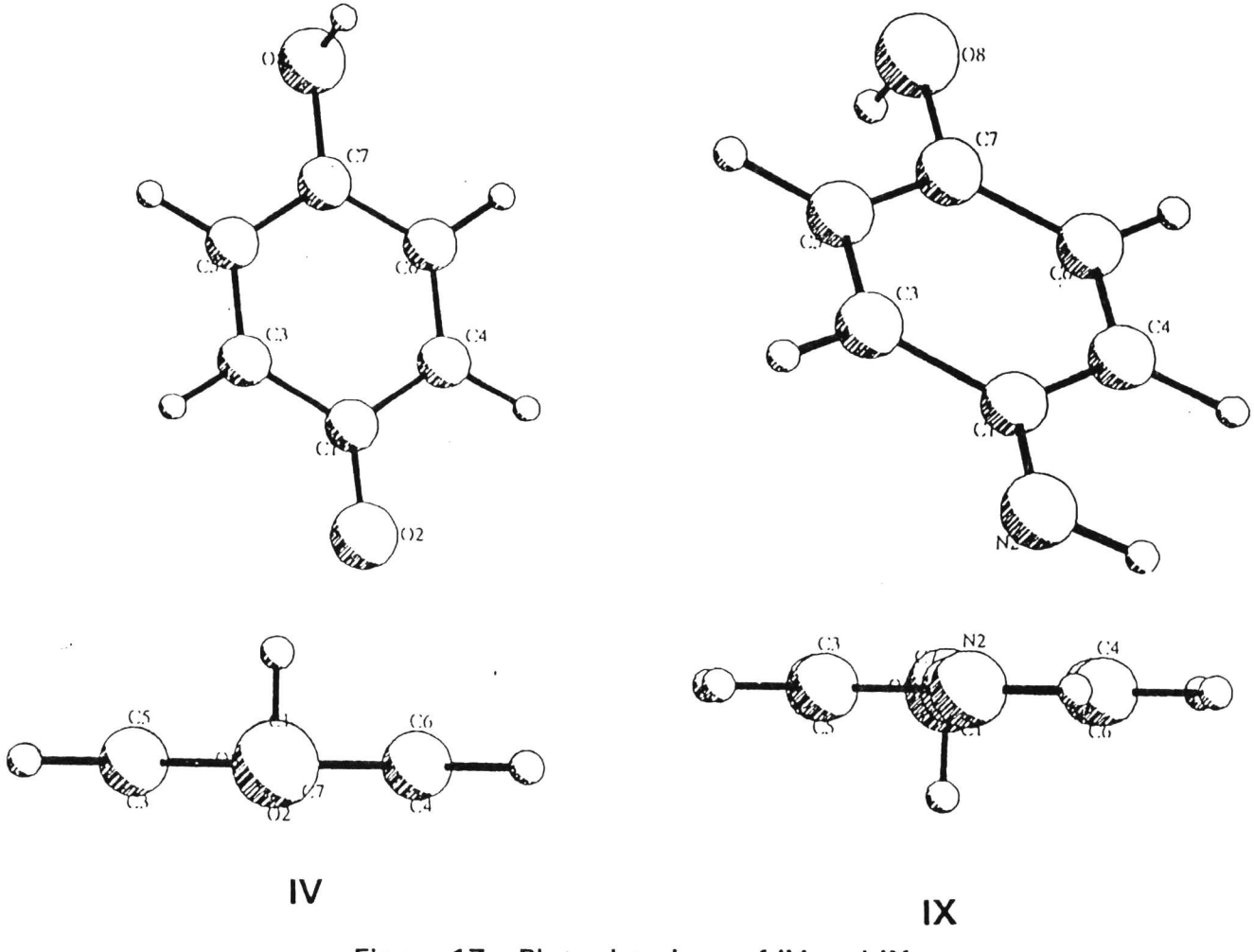

Figure 17. Pluto drawings of IV and IX.

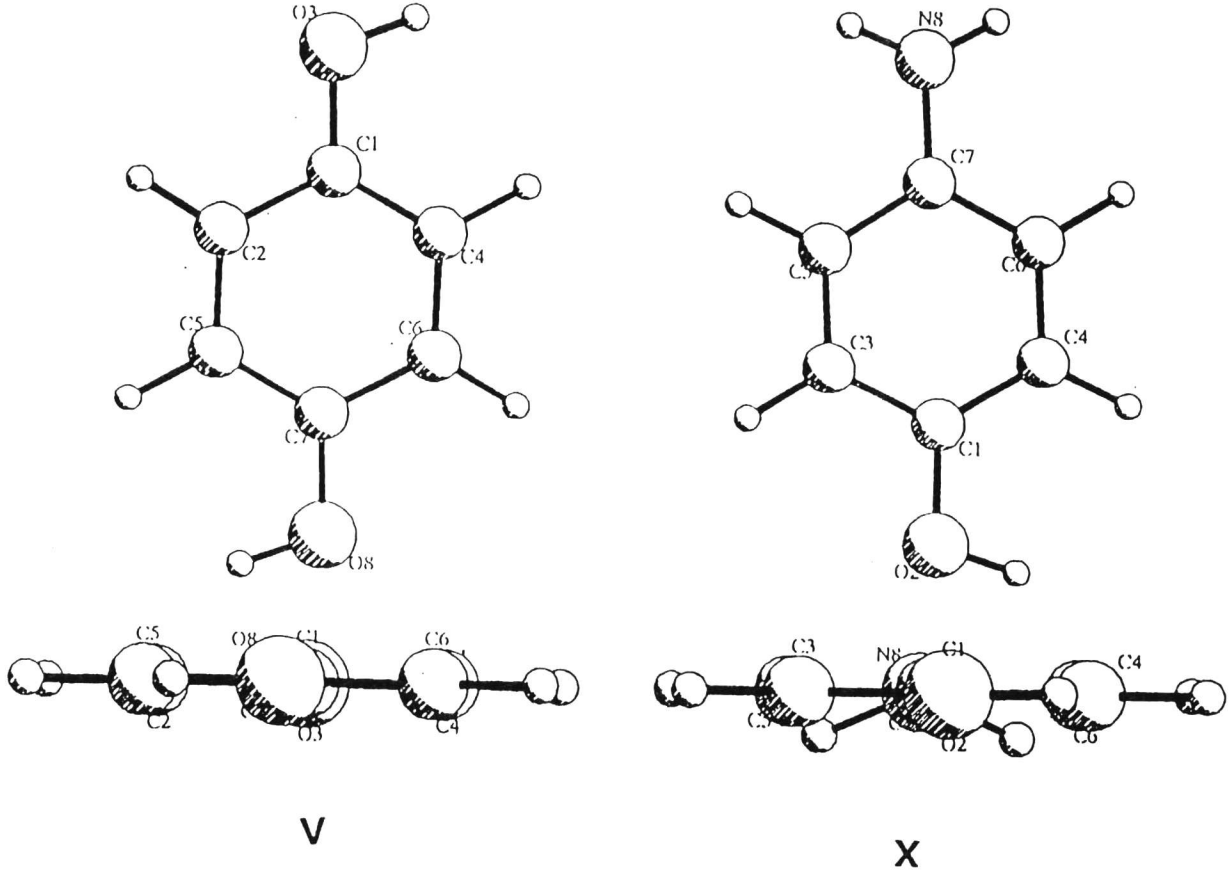

Figure 18. Pluto drawings of V and X.

correlation between transcription inhibition and dissociation rates of drug-DNA correlation between transcription inhibition and dissociation rates of drug-DNA complexes while Straney and Crothers[103] have suggested a correlation between the on-rate of drug-DNA interaction and disruption of the open complex between RNA polymerase and DNA. Both of these reports suggest a role for binding in the mode of action of the anthracyclines. On the other hand, Rizzo et al[104] have reported on the kinetics of association and dissociation of calf thymus DNA and five anthracyclines including adriamycin and daunomycin. They concluded that the correlation of cytotoxicity data with both association and dissociation rates of the complexes was not significant and suggested that other factors must be involved in modulating the different biological properties of the anthracyclines. We thus invoke here that species such as $\mathbf{Q}^{\cdot-}$ and different roamers of $\mathbf{QH}^{\cdot}$ may be responsible for some of the elusive nature of the mode of actions of the anthracyclines. We are currently pursuing the implications of these findings to develop a plausible mode of action for the drug.

Absolute Electronegativity and Absolute Electron Affinity and Chemical Hardness. Table 4 contains the AM1 calculated frontier molecular orbital energies. In this Table, listings of the HOMO, SOMO, and LUMO orbital energies are given for the parent molecules I, VI and XI as well as for their corresponding activated forms. For $Q^{\cdot-}$ and $\mathbf{QH}^{\cdot}$ radicals, values are given for both α and β (in parenthesis) orbitals since there is an unpaired electron in the

Table 4. **AM1 calculated frontier molecular orbital energies for the one-ring systems (Figure 9). Orbital energies given for $Q^{-\cdot}$ and QH^{-} are for α and β (in parenthesis) electrons[a]. Values are given in eV.**

		HOMO	SOMO	LUMO
I		-10.88		-1.74
VI	Q	-10.46		-1.37
XI		-9.77		-1.03
II		-5.53(-5.08)	-2.77(3.89)	4.65(5.57)
VII	Q^{-}	-5.34(-4.26)	-2.59(4.34)	4.87(5.67)
XII		-5.49(-3.50)	-2.41(4.65)	5.01(5.80)
III		-10.94(-10.67)	-9.14(-1.29)	0.12(0.67)
VIII	Q $H^{\cdot}$	-10.62(-10.21)	-8.51(-1.00)	0.42(0.95)
XIII		-10.38(-9.67)	-8.33(-0.30)	0.63(1.04)
IV		-2.84		5.39
IX	Q H^{-}	-2.81		5.48
XIV		-2.31		5.62
V		-8.73		0.22
X	Q H_2	-8.27		0.44
XV		-7.92		0.64

[a]Values for the SOMO energies (in parenthesis) are for unoccupied orbitals. LUMO energies given for $Q^{-\cdot}$ and QH^{-} are for the second highest unoccupied molecular orbital.

SOMO orbital. For radicals, the negatives of the α-orbitaland the β-orbital energies were taken as the ionization potential and the electron affinity,respectively. SOMO energies were used to calculate the molecular parameters for the radical species.

Data from Table 4 suggest that the semiquinone anions IV, IX and XIV should be the most reactive species, based on their orbital energies, followed by the radical anions II, VII and XII. Based on comparison of the orbital energies for the frontier orbitals in Table 4, their reactivity, in decreasing order, follows QH^- > $Q^{\cdot-}$ > QH_2 > $QH^{\cdot}$ > Q for the three systems (I, VI, and XI).

Absolute electron affinities and electronegativities, along with electronic chemical potentials are given in Table 5. It is seem that modest reductions in electron affinity are calculated for the iso-electronic analogs of I. These reductions in electron affinity mean one- and two-electron reductions in VI and XI are less favored. These could have significant implications for biological activity. In those cases in which the biological activity is determined by the reduced forms of the anthracyclines, analogs which lead to reduce electron affinity must be sought to effect changes in biological activity when such activity is undesired. Two such activities, in the case of anthracyclines, are cardiotoxicity and cytotoxicity.

Table 5 also shows the absolute electronegativities of the parent molecules I, VI and XI and their reduced forms. The absolute electronegativity of structures 5 and 6 in Figure 12 are 4.681 and -1.668 eV, respectively, i.e.,

Table 5. Absolute electronnegativities (χ), electron affinities and absolute hardness (η). All values are given in eV.

	I	VI	XI	ORDER
ABSOLUTE ELECTRON AFFINITIES				
Q	1.735	1.372	1.031	I>VI>XI
$Q^{\cdot-}$	-3.891	-4.344	-4.651	I>VI>XI
$QH^{\cdot}$	1.288	0.996	0.295	I>VI>XI
QH^{-}	-5.391	-5.483	-5.620	I>VI>XI
QH_2	-0.219	-0.439	-0.641	I>VI>XI
ABSOLUTE ELECTRONEGATIVTIES(μ)				
Q	6.305	5.917	5.395	I>VI>XI
$Q^{\cdot-}$	-0.560	-0.877	-1.200	I>VI>XI
$QH^{\cdot}$	5.212	4.753	4.312	I>VI>XI
QH^{-}	-1.275	-1.335	-1.655	I>VI>XI
QH_2	4.250	3.915	3.635	I>VI>XI
ABSOLUTE CHEMICAL HARDNESS(η)				
Q	4.57	4.55	4.37	I>VI>XI
$Q^{\cdot-}$	3.33	3.47	3.53	XI>VI>I
$QH^{\cdot}$	3.92	3.76	4.02	XI>I>VI
QH^{-}	4.11	4.14	3.96	VI>I>XI
QH_2	4.47	4.35	4.27	I>VI>XI

the values are relatively close to those in Table 5. Again, the electronegativities of the analogs of I and their respective redox states are calculated for $Q^{\cdot -}$ reduced forms are considerably lower. Interestingly, negative electronegativities and QH^{-}. It is also interesting that the calculated electronegativity of I is 6.035 eV, a value that is comparable to that of O_2(6.2 eV).[88] Assuming everything else to be equal, these values suggest that I can effectively compete with O_2 in a redox couple reaction. This is particularly significant, because it strongly suggests that 1,4-benzoquinone can effectively interfere, for example, with the sequence(s) in the electron-transport chain of a mitochondrion[105] which affects the normal physiological flow of electrons. Using the calculated values, an ordering in electronegativity can be made:

$$O_2 \sim Q > QH^{\cdot} > QH_2 > Q^{\cdot -} > QH^{-}$$

This suggests that $O_2/Q^{\cdot -}$ and O_2/QH^{-} couples are possible leading to formations of $O_2^{\cdot -}$ (superoxide). In light of the presumption that $O_2^{\cdot -}$ is formed by a reaction of O_2 with radical intermediated produced from anthracyclines,[12,36] the redox couples shown to be feasible from the calculations are rather interesting. The calculated values also suggest that Q, $QH^{\cdot}$ and probably QH_2 can be reduced by $Q^{\cdot -}$ and QH^{-}, thus indicating inter- and intramolecular electron transfer reactions are very feasible. Since χ is the negative of μ, the reverse of the decreasing order in absolute electronegativity will give a decreasing order in μ which reflects the decreasing order in escaping tendency of the electrons in the

species. When I and its reduced forms are compared with VI and XI, the respective escaping tendency of the electrons in VI and XI and their reduced forms are greater. Overall, results from the three systems demonstrated that the most electronegative molecule was the benzoquinone system followed by its imine and diimine analogs, respectively.

The AM1 calculated absolute hardness data are also given in Table 5. The data demonstrated that within similar systems, the radical systems (quinone radical anion, semiquinone, and semiquinone radical anion) produced a smaller hardness gaps (decreased values suggest the potential for a more reactive molecule). This suggests that the radical systems are likely to change in electronic character by transferring electrons to other systems (as in the case of molecular oxygen).

Comparing the three isoelectronic systems, Q, QH^-, and QH_2 of the diimine molecule, $QH^{\cdot}$ for the imine, and $Q^{-\cdot}$ for the benzoquinone moiety all gave lower values.

B. COMPARISON OF TWO-RING SYSTEMS

The two-ring systems are displayed in Figure 19. One mode of their reductive activation follow the mechanism displayed in Figure 7 for one-ring systems. Listed in Table 6, are some general parameters calculated by AM1 for these systems. Values include dipole moments, heats of formation (ΔH_f), and ionization potential (IP). Table 7 lists the calculated AM1 electron and proton attachment reaction enthalpies computed from ΔH_f given in Table 6. These reaction enthalpies values are very similar to values computed for the one-ring systems (Table 3). The calculated thermodynamic values for the one- and two-ring systems demonstrated that electron attachment was favorable for the quinone system, whereas proton attachment, semiquinone formation, hydroquinone formation (1-->5) were favorable for the diimine case. The only exception between the two systems were values computed for the semiquinone anion formation (1-->4) and hydroquinone formation (3-->5). The one-ring system data displayed that semiquinone anion formation was favorable for p-benzoquinone imine followed by benzoquinone, and p-benzoquinone diimine systems. The two-ring systems demonstrated semiquinone anion formation was favorable for the quinone systems followed by the diimine- and imine-systems. Hydroquinone formation was favorable for the diimine moiety followed by imine- and quinone moieties. Table 8 gives all AM1 calulated frontier molecular orbital energies for the two-ring systems. Again, trends seen for these systems were similar to those for the one-ring systems. Molecular

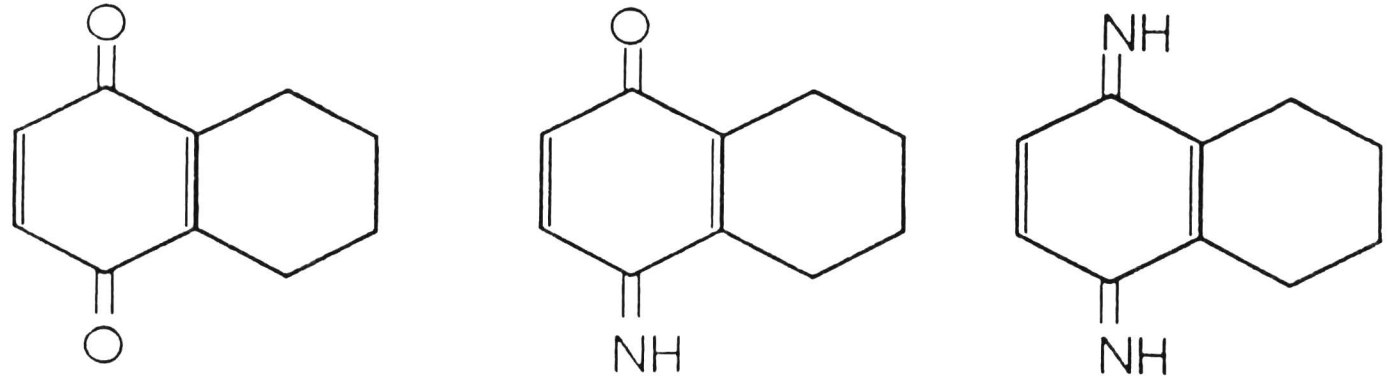

Figure 19. Structures of two-ring systems I, VI, XI.

Table 6. **General parameters as calculated by AM1 for the two-ring systems given in Figure 19.**

Structure[a]	ΔH_f(kcal/mol)	Dipole(debyes)	IP(eV)
I	-47.40	0.71	10.22
II	-97.89	4.50	2.79
III	-63.46	3.41	8.92
IV	-107.6	6.43	2.88
V	-85.73	2.77	8.60
VI	1.65	2.66	9.95
VII	-43.52	5.70	2.61
VIII	-16.42	3.32	8.68
IX	-47.33	6.65	2.40
X	-42.78	2.02	8.18
XI	52.27	3.16	9.50
XII	13.31	6.30	2.43
XIII	25.66	3.38	8.22
XIV	-2.16	7.52	2.38
XV	0.35	0.18	7.84

[a] Structures I-->V are for 1,4-benzoquinone (I) and its reductively activated states (II-->V). II is the quinone anion, III is the semiquinone radical, IV is the semiquinone radical anion, and V is the hydroquinone system. Systems VII-->X are imine analog (VI) activated forms (given in the same order as above) and XII-->XV are the diimine analog (XI) with activated states.

Table 7. **AM1 calculated electron and proton attachment reaction enthalpies (ΔH_{rxn})[a] for two-ring systems (Figure 19).**

Process	I	VI	XI	ORDER[b]
Electron Attachment				
1------>2	-50.49	-45.18	-38.96	I>VI>XI
3------>4	-44.18	-30.91	-27.82	I>VI>XI
Proton Attachment				
2------>3	34.43	27.10	12.35	XI>VI>I
4------>5	21.90	4.55	2.51	XI>VI>I
Semiquinone Formation				
1------>3	-16.06	-18.08	-26.61	XI>VI>I
Semiquinone Anion Form.				
1------>4	-60.23	-48.99	-54.43	I>XI>VI
Hydroquinone Formation				
1------>5	-38.33	-44.44	-51.93	XI>VI>I
3------>5	-22.27	-26.36	-25.31	VI>XI>I

[a] Reduction processes involving electron and proton attachments pertain to scheme as in Figure 7.
[b] Order given for decreasing stability.

Table 8. **AM1 calculated frontier molecular orbital energies for two-ring systems (Figure 19). Orbital energies given for $Q^{-\cdot}$ and $QH^{\cdot}$ are α and β (in parenthesis) electrons.**

		HOMO	SOMO	LUMO[b]
I[a]		-10.22		-1.59
VI	Q	-9.95		-1.21
XI		-9.50		-0.94
II		-5.49(-4.93)	-2.79(3.78)	4.46(5.36)
VII	$Q^{-\cdot}$	-5.38(-4.27)	-2.61(4.22)	4.66(5.45)
XII		-5.26(-3.56)	-2.43(4.50)	4.77(5.56)
III		-10.24(-10.11)	-8.92(-1.14)	0.22(0.74)
VIII	$QH^{\cdot}$	-10.04(-9.90)	-8.68(-0.41)	0.41(0.84)
XIII		-9.81(-9.45)	-8.22(-0.22)	0.66(1.05)
IV		-2.88		5.12
IX	QH^{-}	-2.40		5.24
XIV		-2.38		5.29
V		-8.60		0.25
X	QH	-8.18		0.43
XV		-7.84		0.61

[a] I, VI, and XI are the quinone, imine-, and diimine- two ring systems. II, VII, and XII are the quinone radical anions, III, VIII, and XIII are semiquinone radicals, IV, IX, and XIV are the semiquinone anions, and V, X, XV are the respective hydroquinone systems for the two-ring systems, respectively.

[b] LUMO energy values given for $Q^{-\cdot}$ and QH^{-} are for second highest occupied energy level. SOMO energies located in parenthesis are unoccupied molecular orbitals.

orbital data demonstrated that the semiquinone anions IV, IX, and XIV should have been the most reactive systems, followed by the radical anions II, VII, and XII. Orbital energy data showed that reactivity in decreasing order, follow $QH^- > Q^{\cdot-} > QH_2 > QH^{\cdot} > Q$ for the three systems shown in Figure 19.

Table 9 lists molecular parameters calculated from AM1 frontier molecular orbital energies. Electronegativity values determined from calculations followed the exact trend observed in the one-ring case. Negative values were calculated for $Q^{\cdot-}$ and QH^-. Comparable to the one-ring case, the calculated value of I (5.9) was similar to the experimental value computed for molecular oxygen. This is important because it suggests that the quinone system may interfere with electron-transport reactions which are speculated to occur between anthracyclines and molecular oxygen.

Absolute hardness values are also given in Table 9 for the two-ring systems. Values (inter-system) were somewhat different from the one-ring systems. Data demonstrate that within a set of redox states, smaller orbital energy gaps were observed for radical systems $Q^{\cdot-}$ and $QH^{\cdot}$ and for the QH^- intermediate of all three molecules (similar to one-ring systems). The order of reactivity (decreasing) for each system was: for the benzoquinone (I) group of redox states, $Q^{\cdot-} > QH^{\cdot} > QH^- > Q > QH_2$; for the imine (VI) and the diimine (XI) group of redox states, $Q^{\cdot-} > QH^- > QH^{\cdot} > QH_2 > Q$;

Comparing the three different systems, orbital energy (for the radical systems) gaps were smaller in magitude for: Q and QH_2 of the diimine moiety,

Table 9. **Molecular parameters calculated using AM1 frontier molecular orbital energies. Values are given for chemical hardness (η) and electronegativity (χ). Values listed are given for the two-ring systems (Figure 19).**

Chemical Hardness

		I	VI	XI
Q	4.28	4.37		VI > I > XI
$Q^{-\cdot}$	3.28	3.41	3.46	XI > VI > I
$QH^{\cdot}$	3.89	4.13	4.00	VI > XI > I
QH^{-}	4.00	3.82	3.84	I > XI > VI
QH_2	4.42	4.31	4.13	I > VI > XI

Electronegativity

		I	VI	XI
Order				
Q	5.91	5.58	5.21	I > VI > XI
$Q^{-\cdot}$	-0.49	-0.80	-1.03	I > VI > XI
$QH^{\cdot}$	5.03	4.55	4.22	I > VI > XI
QH^{-}	-1.12	-1.42	-1.45	I > VI > XI
QH_2	4.17	3.88	3.61	I > VI > XI

$Q^{\cdot}$ and $QH^{\cdot}$ of the benzoquinone moiety, and QH^{-} of the imine moiety. This suggest that the addition of the second ring may have some influence on the overall reactivity of the system. From parameters determined (electronegativity, electron affinity, and molecular orbital energies), second ring addition did not influence the overall reactivity of the reductively activated systems.

C. COMPARISON OF DIHYDROXY-1,4-NAPHTHAQUINONE AND ITS IMINO ANALOG

Electron and Proton Attachments in Dihdroxy-1,4-Naphthaquinone and Its Analog. 5,8-Dihydroxy-1,4-naphthaquinone (I) and its analog, dihydroxy-1,4-naphthaquinone imine (VI) are displayed in Figure 20. Out of all systems investigated thus far, these systems should best model possible reactivity for the anthracycline drug class because of second ring substitution. Reaction enthalpies data for processes of electron and proton attachments give a basic overview of reduction enthalpies which may occur with these systems. Once again, the reduction of these systems to activated intermediates follow the mechanism displayed for the one-ring case (displayed in Figure 7).

Figures 21-23 demonstrate possible reductive routes for VI (a)-(c) Reaction enthalpies values calculated for these systems (along with their activated species) given in Table 11 are for the following reaction sequence:

$$Q \text{--} > Q^{\cdot-} \text{--} > QH^{\cdot} \text{--} > QH^{-} \text{--} > QH_2$$

1 2 3 4.

Where 1 and 3 are electron attachments steps and 2 and 4 are proton attachments steps. Within each system (napthaquinone and its imine analog), electron attachments were favorable, where the addition of the first electron was highly favored. Data from reaction enthalpies data given in the Table 10 demonstrated how characteristics observed for the one- and two-ring cases (discussed earlier) are similar for their dihydroxy conterparts. Comparing

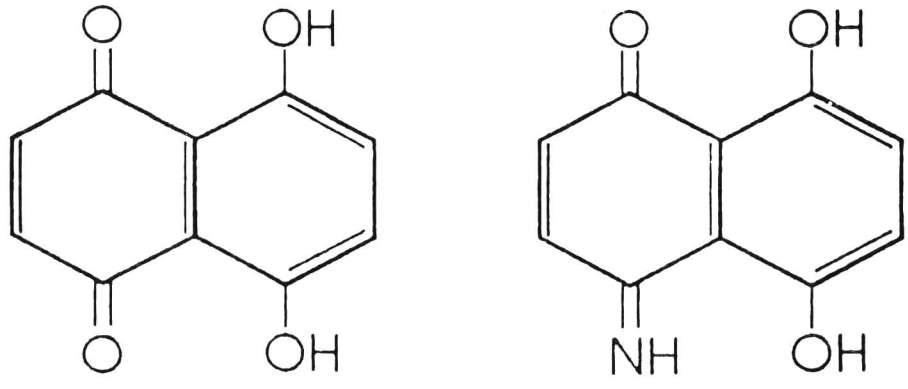

I. VI.

Figure 20. Structures of 5,8-dihydroxy-1,4-napthaquinone (I) and its imine-analog (VI).

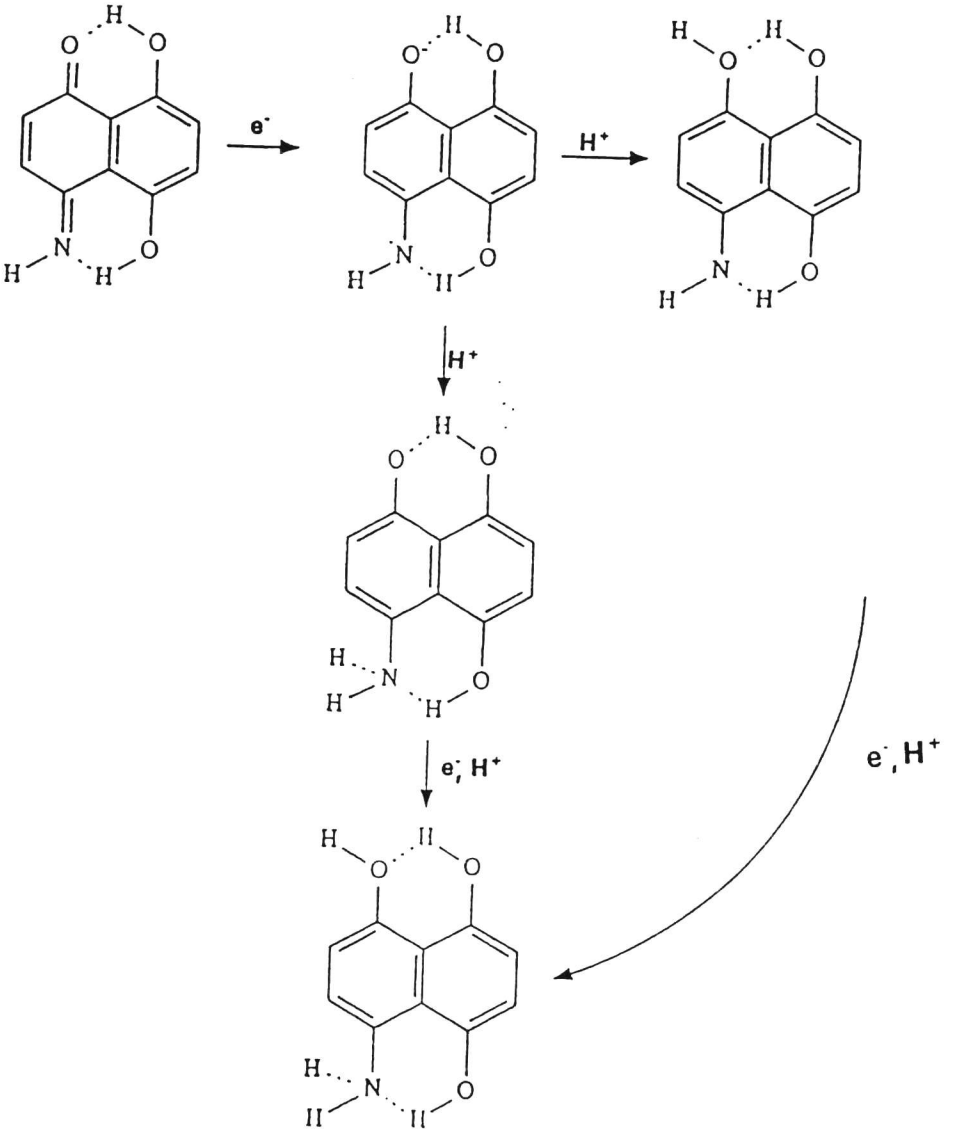

Figure 21. Possible reductive routes of VI(a).

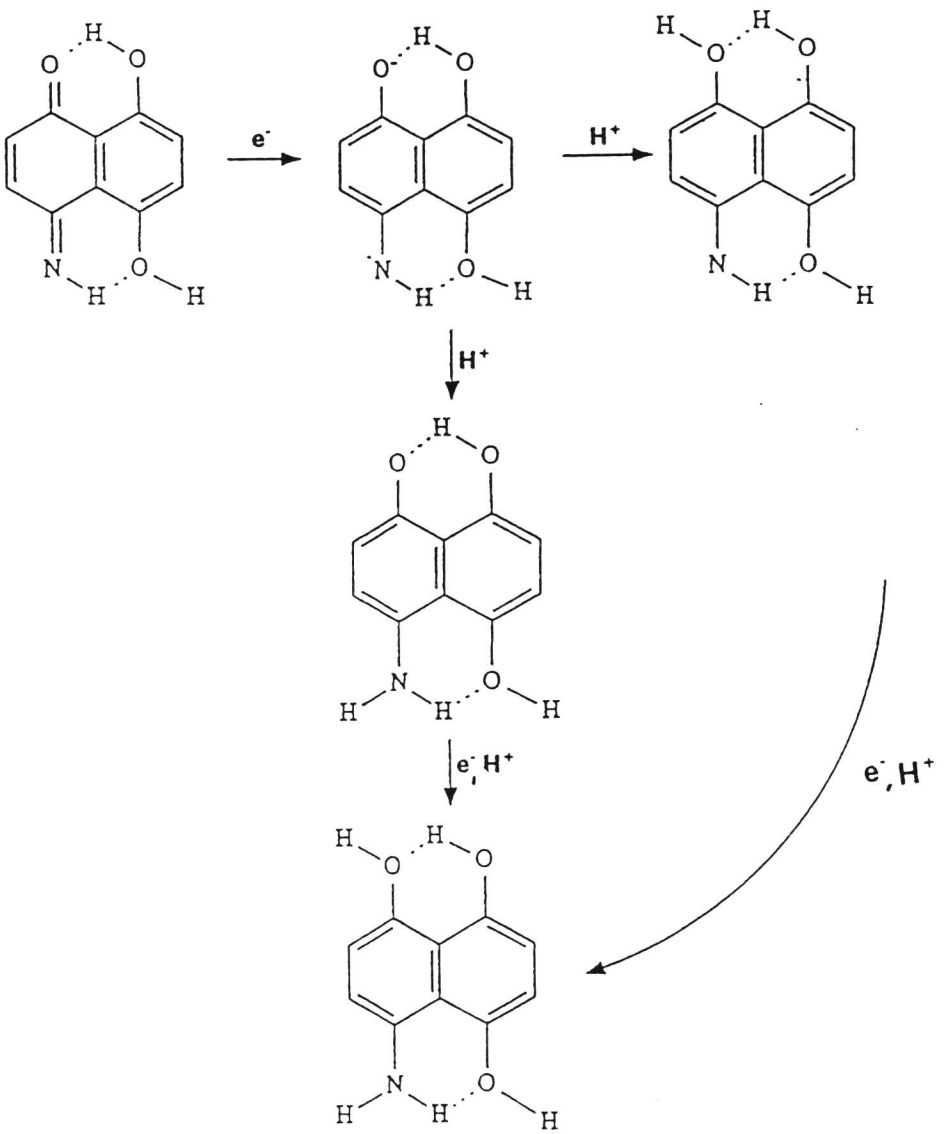

Figure 22. Possible reductive routes of VI(b)

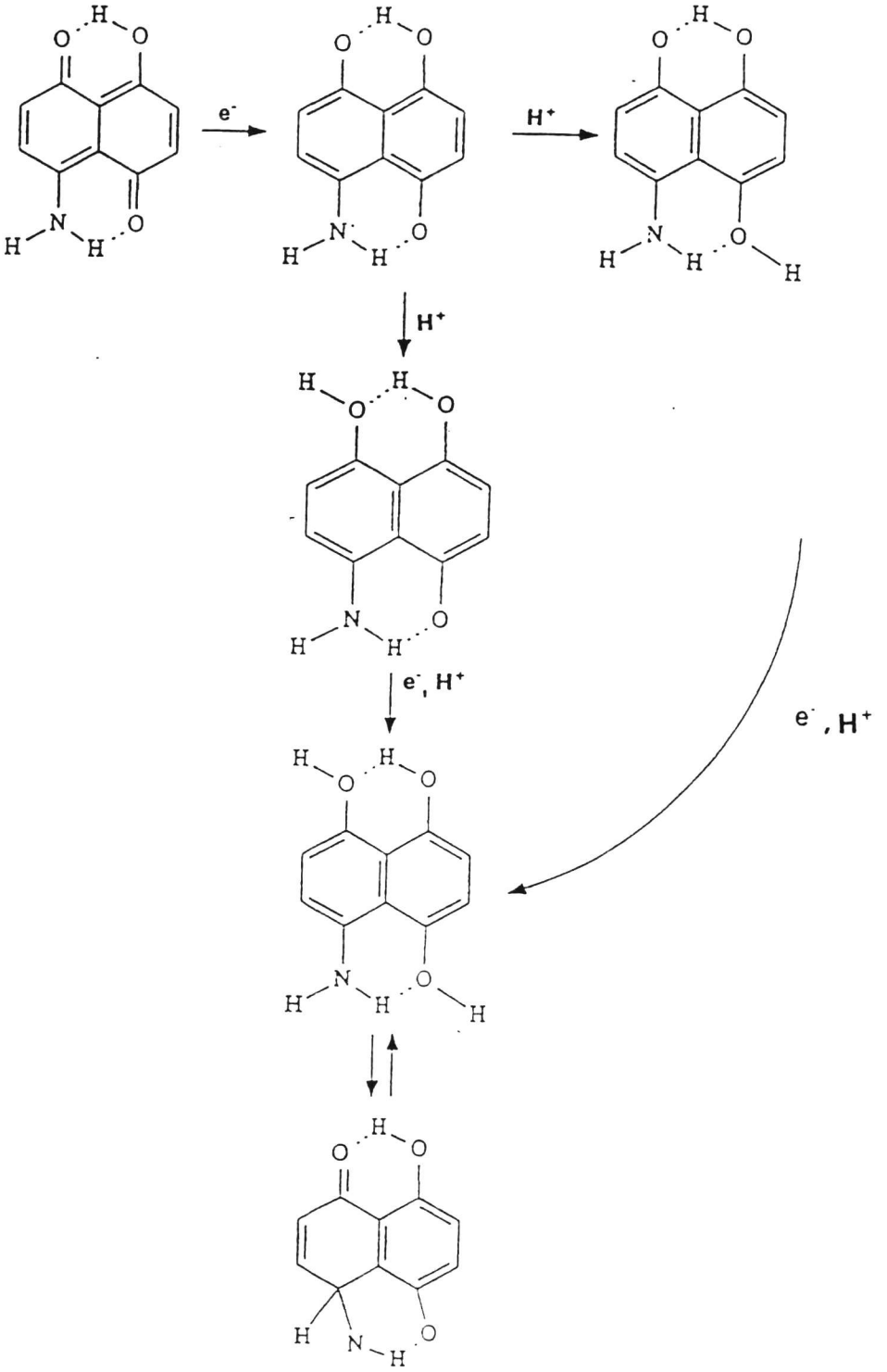

Figure 23. Possible reductive routes of VI (c).

Table 10. Reaction enthalpies (kcal/mol) for electron and proton attachment steps and for the overall conversion of Q --> QH_2. Values are for systems displayed in Figures 21-23.

I)	1	2	3	4	ORDER	OVERALL
I	-56.2	44.7	-49.7	37.4	1<3<4<2	-23.8
VI(a)	-49.3	26.9	-38.4	28.7	1<3<2≅4	-32.1
	-49.3	35.9	-32.6	13.9	1<3<4<2	-32.1
VI(b)	-52.9	40.9	-41.6	26.4	1<3<4<2	-27.2
	-52.9	39.5	-38.8	24.9	1<3<4<2	-27.2
VI(c)	-56.3	35.8	-38.4	28.7	1<3<4<2	-30.2
	-56.3	36.8	-41.2	30.5	1<3<4<2	-30.2

systems, electron attachment (steps 1 and 3) were favorable for I followed by VI. Proton attachments (steps 2 and 4) were favorable for the imino-systems. These trends were observed in the first two cases for the one and two ring systems which again suggested that replacement of O by NH in the quinone moiety made proton attachments favorable (steps 2 and 4), electron attachment less favorable, and trends observed for hydroquinone formation followed that of proton attachment. This data in addition to data observed for the first two systems (one- and two-ring systems) show the relative importance of electron and proton attachment steps in the reductive activation of quinone and its isoelectronic analog.

Absolute Electronegativity and Chemical Hardness of Dihydroxy-1,4-Naphthaquinone and its Imine Analog. These values along with AM1 calculated frontier molecular orbital energies are given in Table 11. LUMO energies values for $Q^{-\cdot}$ and $QH^{\cdot}$ are given for the β electron SOMO energy. Data observed from the frontier molecular orbital energies in the Table suggest that the semiquinone anions (QH^{-}) for both systems should yield to be the most reactive. These values are followed directly by that of the quinone anion radical ($Q^{-\cdot}$) for the two systems. Based on comparison of orbital energies, reactivity (in decreasing order) followed that of $QH^{-} > Q^{-\cdot} > QH_2 > QH^{\cdot} > Q$ for both systems.

Table 11. **AM1 calculated heats of formation (ΔH_f), Orbital energies (HOMO, SOMO, LUMO), absolute electronegativies (χ) and chemical hardness (η) for systems displayed in Figures 21-23.**

	Redox State	ΔH_F (Kcal/mol)	HOMO(ev)	LUMO(ev)[a]	χ(ev)	η(ev)
I	Q	-105.8	-9.20	-1.79	5.46	3.71
	$Q^{-\cdot}$	-162.1	-3.13	3.03	0.13	3.07
	$QH^{\cdot}$ (1)	-117.4	-8.59	-1.51	5.05	3.54
	QH^{-} (1)	-167.1	-3.12	4.02	-0.45	3.57
	QH_2	-129.7	-7.90	-0.42	4.16	3.74
VI(a)	Q	-53.10	-9.11	-1.35	5.23	3.88
	$Q^{-\cdot}$	-102.3	-2.80	3.74	-0.47	3.27
	$QH^{\cdot}$ (1)	-75.4	-7.95	-1.07	4.51	3.44
	QH^{-} (1)	-113.8	-2.59	4.16	-0.79	3.37
	QH_2	-85.2	-7.46	-0.12	3.79	3.67
	$QH^{\cdot}$ (2)	-66.4	-8.44	-0.59	4.51	3.93
	QH^{-} (2)	-99	-2.55	4.20	-0.83	3.38
VI(b)	Q	-52.5	-8.87	-1.50	5.19	3.69
	$Q^{-\cdot}$	-105.4	-2.99	3.49	-0.25	3.24
	$QH^{\cdot}$ (1)	-64.5	-8.20	-1.20	4.70	3.50
	QH^{-} (1)	-106.1	-2.76	4.14	-0.69	3.45
	QH_2	-79.7	-7.89	-0.45		
	$QH^{\cdot}$ (2)	-65.9	-8.41	-0.87	4.64	3.77
	QH^{-} (2)	-104.7	-2.77	4.16	-0.70	3.46
VI(c)	Q	-55	-8.28	-1.72	5.00	3.28
	$Q^{-\cdot}$	-111.3	-3.11	3.00	0.06	3.05
	$QH^{\cdot}$ (1)	-75.4	-7.95	-1.07	4.51	3.44
	QH^{-} (1)	-113.8	-2.59	4.18	-0.79	3.37
	QH_2	-85.2	-7.46	-0.12	-3.79	3.67
	$QH^{\cdot}$ (2)					
	QH^{-} (2)					

[a] Values given in the LUMO column for $Q^{-\cdot}$ and QH^{-} are SOMO energies computed from AM1.

Also given in Table 11, are the molecular parameters absolute electronegativity and chemical hardness (electronic chemical potential was excluded because it gives the same information as electronegativity). The electronegativity values for the quinone moiety decrease in the following order: $Q > QH^{\cdot} > QH_2 > Q^{-\cdot} > QH^{-}$. This suggest that the quinone species is the least likely culprit and the semiquinone anion species is the most likely candidate to give up electrons through electron-transfer reaction (i.e. to molecular oxygen). Electronegativity trends observed for the analog (a, b, and c) followed that of the quinone case (Note: QH_2 value was not obtained for b). Comparing the two systems, electronegativity data demonstrated that all species ($Q \text{--} > QH_2$) gave results where values for I were greater than that computed for VI in each case. These data show that electronegativity values decreased when the keto group (=O) was substituted with an imine group (=NH). This suggests that because of the imine substitution, electron-transfer reactions should proceed more readily when reductively activated states interact with molecular oxygen.

Chemical hardness trends followed the order: $Q^{-\cdot} < QH^{\cdot} < QH^{-} < Q < QH_2$ for the quinone system, $Q^{-\cdot} < QH^{-} < QH^{\cdot} < QH_2 < Q$ for its (a) and (b) analogs (again note that a value was not obtained for QH_2); and $Q^{-\cdot} < Q < QH^{-} < QH^{\cdot} < QH_2$ for the (c) analog. The only difference observed from calculation for these systems (VI a--> c) were proposed hydrogen-bonding mechanisms. Differences seen for VIc could have resulted in the hydrogen-bonding mechanism proposed because of the conformational orientation of the hydrogen atoms on the molecule.

Comparing chemical hardness values (in decreasing order) for the two systems, data indicated that all imine systems gave lower values which consequently suggested that these species should be more reactive compared to the parent napthaquinone system.

D. COMPARISON OF ONE- AND TWO-RING QUINONES

Does ring or substituent additions to the benzoquinone molecule display differences in reactivity? That was the last question investigated in this study. To determine if ring and/or substituent additions had any effect on the overall reactivity of one- and two-ring benzoquinone/napthaquinone systems, systems listed in Figure 24 were subjected to a comparative study. Reactivity of each was compared based on absolute electronegativity, chemical hardness, and reaction enthalpies. There were a total of four benzoquinone/napthaquinone systems investigated in this section (structures displayed in Figure 24).

Comparison of Relative Reaction Enthalpies for the Quinone Systems. The calculated reaction enthalpies for electron (steps 1 and 3) and proton (steps 2 and 4) attachments are given in Table 12 for systems I to IV. All systems are of the quinone form and one mode of reductive activation was modeled by the following process:

$$Q \text{--} > Q^{\cdot-} \text{--} > QH^{\cdot} \text{--} > QH^{-} \text{--} > QH_2$$

$$1 \quad 2 \quad 3 \quad 4$$

where 1 and 3 are electron attachments steps and 2 and 4 are proton attachments steps. The data suggest that within each system, the order for which the process should proceed was favorable for steps 1 and 3 (formations of the quinone anion and semiquinone anion). Steps 2 and 4 (formations of semiquinone radical and hydroquinone) were not favored. This data seem valid

Figure 24. One- and two-ring quinones.

TABLE 12. Reaction enthalpies (kcal/mol) for the electron and proton attachment steps and for the overall conversion of Q→QH_2 (for systems displayed in Figure 24).

	1	2	3	4	Overall
I	-51.8	35.4	-45.1	20.9	-40.6
II	-49.1	35.9	-43.3	28.7	-27.8
III	-53.2	40.0	-49.1	35.8	-26.5
IV	-56.2	44.7	-49.7	37.4	-23.8

because of the electronegative character found on these systems (oxygen atoms are very electronegative which should attract electrons). Comparing the four systems, data demonstrated that electron attachments were favorable for thedihydroxy case and proton attachments were favorable for the benzoquinone molecule. The overall formation of hydroquinone from the benzoquinone systems was favorable for the benzoquinone moiety (I) and the thermodynamic values (in decreasing order) $1<2<3<4$, presented less favorable results (compared to the one-ring systems).

Electronegativity and Chemical Hardness. These values are given in Table 13. The trend for electronegativity (decreasing) followed that of $Q > QH^{\cdot} > QH_2 > Q^{-\cdot} > QH^{-}$ for all four systems. This suggest that regardless of any additions to the benzoquinone system the electronegativity trend observed for all reductively activated quinone systems should follow the same pattern within a family of redox sataes. Comparing the four systems (I-->IV): Q, for the one-ring system, was the most electronegative system, decreasing as the substitution increased; $Q^{-\cdot}$ and QH^{-} of IV, were the most electronegative systems with electronegativity decreasing as substitution decreased; $QH^{\cdot}$ of I, was the most electronegative system, followed by III, IV, and II, respectively; and QH_2 of II was the most electronegative system, followed by that of III, I, and IV, respectively.

Absolute hardness values are also given in Table 13. The trends for

TABLE 13. AM1 calculated heats of formation (ΔHf), orbital energies (HOMO, SOMO, LUMO), absolute electronegativies (χ) and absolute hardness (η) for systems in Figure 24.

	Redox State	ΔH_f	HOMO	LUMO[a]	χ	η
I	Q	-25.1	-10.876	-1.735	6.305	4.571
	$Q^{-\cdot}$	-76.9	-2.771	3.891	-0.56	3.331
	$QH^{\cdot}$	-41.5	-9.137	-1.288	5.212	3.925
	QH^{-}	-86.6	-2.844	5.391	-1.275	4.118
	QH_2	-65.7	-8.725	0.219	4.253	4.472
II	Q	-15.9	-10.257	-1.547	5.902	4.355
	$Q^{-\cdot}$	-65	-2.755	3.445	-0.345	3.100
	$QH^{\cdot}$	-29.2	-8.74	-1.205	4.973	3.768
	QH^{-}	-72.5	-2.801	4.226	-0.713	3.514
	QH_2	-43.8	-8.24	-0.491	4.366	3.875
III	Q	-61.4	-9.621	-1.675	5.648	3.973
	$Q^{-\cdot}$	-114.6	-2.969	3.258	-0.145	3.114
	$QH^{\cdot}$	-74.6	-8.865	-1.463	5.164	3.701
	QH^{-}	-123.7	-3.069	4.036	-0.484	3.553
	QH_2	-87.9	-8.154	0.431	4.293	3.862
IV	Q	-105.8	-9.201	-1.788	5.495	3.707
	$Q^{-\cdot}$	-162.1	-3.132	3.003	0.129	3.068
	$QH^{\cdot}$	-117.4	-8.595	-1.507	5.051	3.544
	QH^{-}	-167.1	-3.123	4.018	-0.448	3.571
	QH_2	-129.7	-7.903	-0.424	4.164	3.740

[a] LUMO energy values given in column are for $Q^{-\cdot}$ and $QH^{\cdot}$ are SOMO energy values.

chemical hardness were different in each quinone system. The data demonstrated that for each system, chemical hardness followed the trend (in order of decreasing reactivity): for I, $Q^{-\cdot} < QH^{\cdot} < QH^{-} < QH_2 < Q$; for II and III, $Q^{-\cdot} < QH^{-} < QH^{\cdot} < QH_2 < Q$; and for IV, $Q^{-\cdot} < QH^{\cdot} < QH^{-} < Q < QH_2$. Although trends are not the exact same in each case, all systems show that the intermediates, $Q^{-\cdot}$, $QH^{\cdot}$, and QH^{-} were the most reactive species. Based on chemical hardness data **Q**, $Q^{-\cdot}$, $QH^{\cdot}$, and QH_2 of IV should be the most reactive. For the QH^{-}'s, the most reactive system was that of II. Overall, this data demonstrated that the larger systems are most reactive based on HOMO-LUMO gaps (hardness). Where values, in general, decreased as the substitution and/or ring addition increased.

E. CORRELATION OF ELECTRONIC PROPERTIES WITH EXPERIMENTAL REDUCTION POTENTIALS

Ranghino and Fosi[83] investigated the relationship between frontier molecular orbital energies and redox potential in hopes of elucidating possible structure-activity correlations. They conducted Ab initio studies on anthracyclines differing by redox potential and cardiotoxicity. Correlation of redox potential and electronic distribution in each system was investigated and results demonstrated that HOMO-LUMO gap values with reduction potential gave good results. They concluded that the redox potential values of the chromophore could be compared to the HOMO-LUMO gap. In another study (quinone-unrelated, but supportive information), a correlation study of reduction potential (taken from cyclic voltammograms) of cyanine dyes with their calculated SOMO orbital energies was conducted by Ahmad and Astin.[105] Three approaches (particle-in-a-box, simple Huckel, and MNDO methods) were performed to obtain electron affinities from orbital energies. They concluded that experimental reduction potential values correlated well with quantum mechanical approaches ($r = 0.998$). This study was conducted to demonstrate how biological activity could be correlated to molecular orbital energy data.

Hodnett and coworkers[80] investigated twelve substituted 1,4-naphthaquinones displaying a range of electronic and lipophilic characteristics in order to elucidate their mechanisms of action as antitumor agents. Redox potentials of each was determined. They have found correlations between

biological activity of various quinones with their experimental redox potential. In addition, studies have demonstrated that redox potential may be related to parameters computed from molecular orbital energies, in particular the chemical hardness (HOMO-LUMO gap).[84] To determine if the approach taken in this theoretical investigation gave resonable results, the twelve systems examined by Hodnett's group were subjected to the semiempirical approach and the calculated theoretical parameters were correlated with experimental reduction potentials (systems are located in Figure 25). These values were used to determine the relevance of the semiempirical computational approach taken in this study. Correlation coefficients were obtained using a least squares linear regression approach using the Sigma Plot statistical program.[82] Parameters used in the linear regression analysis were electronegativity, heats of reaction for electron attachments, chemical hardness, and LUMO and SOMO energies (all values are given in Table 14). All parameters were correlated with the experimental reduction potential.

Figure 26 displays plots of reduction potential versus LUMO energies. A correlation coefficient of 0.400 was obtained when all LUMO energies and reduction potential values were used. A correlation coefficient of 0.820 was obtained when three points were excluded (reduction potentials -0.164, -0.165, and -0.224 corresponding to R'/R" substituents (structure #, Figure 25) H/H (1), Cl/$NHCOCH_3$ (8), and CH_3/H (10). Out of all possibilities, exclusion of these systems from the analysis gave the best fit regression line. Of the

SYSTEM	R′	R"
1	H	H
2	OH	C_5H_9
3	Cl	NHC_6H_5
4	Cl	Cl
5	Cl	NH_2
6	Cl	OCH_3
7	Cl	OC_2H_5
8	Cl	$NHCOCH_3$
9	OH	H
10	CH_3	H
11	OCH_3	H
12	Cl	O-n-C_3H_7

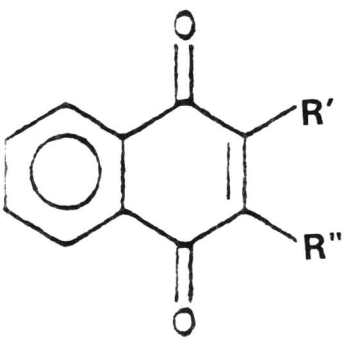

Figure 25. Disubstituted 1,4-napthaquinones.

TABLE 14. Various AM1 calculated values for disubstituted 1,4-naphathaquinones (1-12).

Reduction Potential(eV)[a]	χ (eV)	LUMO (eV)	SOMO (eV)	η (eV)	ΔH_{rxn} (kcal/mol)
-0.164	5.902	-1.547	-2.755	4.355	-53.20
-0.347	5.704	-1.619	-3.026	4.085	-52.97
-0.272	5.161	-1.655	-3.431	3.506	-54.70
-0.146	6.123	-1.890	-3.298	4.233	-59.17
-0.382	5.284	-1.509	-2.881	3.775	-50.21
-0.184	6.040	-1.759	-3.151	4.231	-56.03
-0.192	5.621	-1.665	-3.132	3.956	-54.95
-0.165	5.643	-1.563	-3.248	4.080	-54.42
-0.330	5.926	-1.673	-2.976	4.257	-53.09
-0.224	5.850	-1.493	-2.741	4.362	-48.34
-0.283	5.736	-1.561	-2.912	4.175	-51.08
-0.195	5.993	-1.734	-3.166	4.259	-56.11

[a] Values for reduction potential were taken from reference 83.

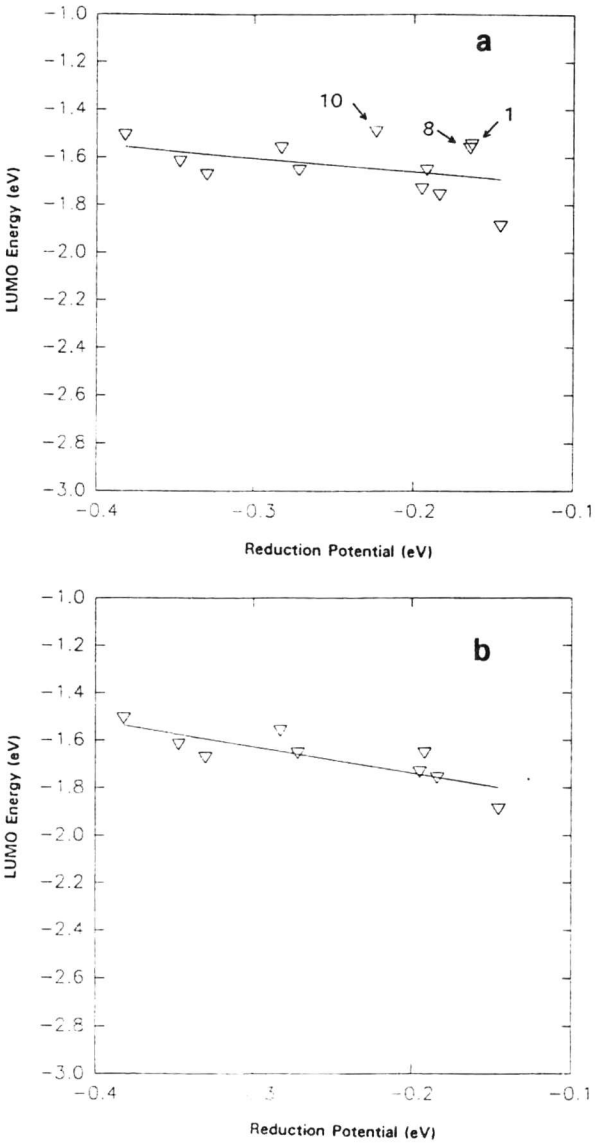

Figure 26. Plots of LUMO energies vs. reduction potential for disubstituted 1,4-napthaquinone systems (1-12, Figure 25). The plot in a is obtained by performing the regression analysis on all 12 points. The plot in b is obtained by excluding the points indicated by the arrows in a.

excluded systems (from regression analysis) 1 and 10 have simple substituents for R' and R" while 8 has a complex substituent for R". The R' substituents for systems 1 and 10 were different from the ten remaining systems in that the other systems had substitutions where either one or both of the substituents were electronegative.

Figure 27 displays the plots of the heats of reaction versus reduction potential for electron attachment. A correlation of 0.567 was obtained when all values were included in the regression analysis. A value of 0.879 was generated when the values (corresponding to the same three systems 1, 8, 10) were excluded as in the LUMO energy case. Out of all possibilities, exclusion of the same three values (seen in the LUMO case) gave the best fit. This suggests that either LUMO energies and/or heats of reaction for electron attachment values could be used as parameters to relate molecular orbital energies to biological activity.

Absolute hardness versus reduction potential plots are located in Figure 28. Linear regression data (correlation coefficients) obtained for this set was not as good as demonstrated for the LUMO energies and heats of reation for electron attachment plots. The first plot displays linear regression data for all points obtained from analysis. The correlation coefficient when all points were included in the regression analysis was 0.411. A correlation coefficient of 0.725 was obtained for the best fit line with three points excluded (displayed in the second plot).

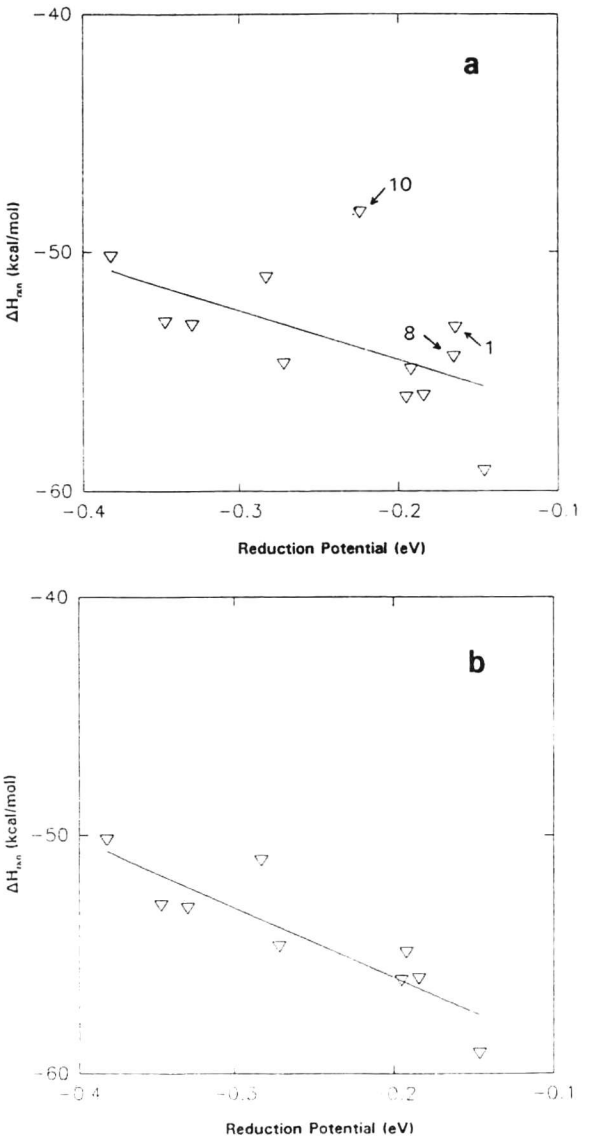

Figure 27. Plots of heats of reaction vs. reduction potential for disubstituted 1,4-naphthaquinone systems (1-12, Figure 25). The plot in a is obtained by performing the regression analysis on all 12 points. The plot in b is obtained by excluding the points indicated by the arrows in a.

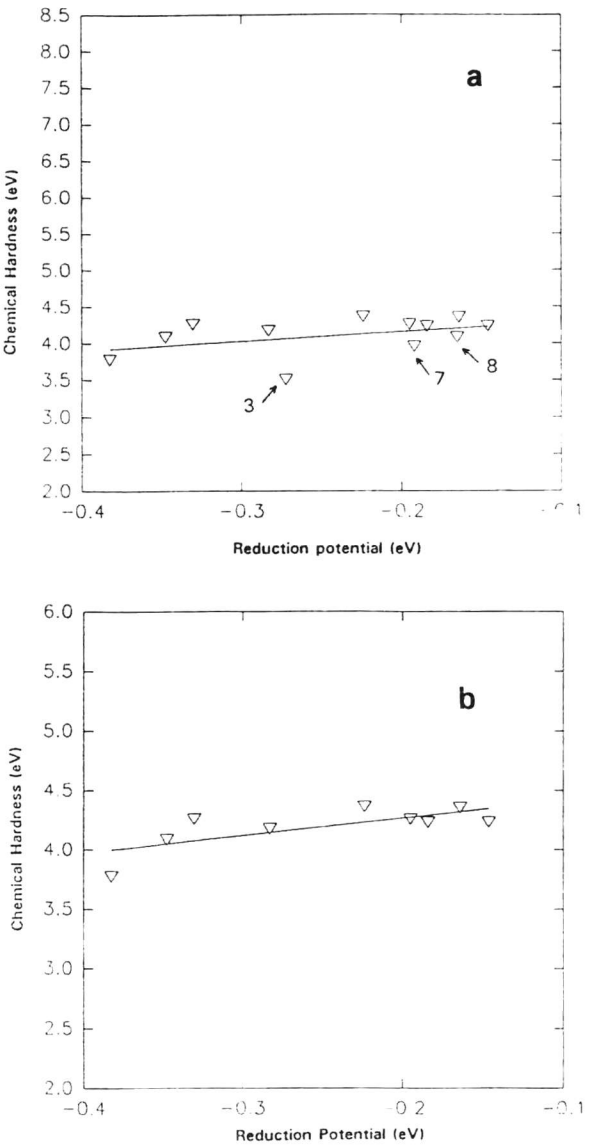

Figure 28. Plots of absolute hardness vs. reduction potential for disubstituted 1,4-naphthaquinone systems (1-12, Figure 25). The plot in a is obtained by performing the regression analysis on all 12 points. The plot in b is obtained by excluding the points indicated by the arrows in a.

Points corresponding to reduction potentials of -0.165, -0.272 and -0.192 (systems 3, 7, and 8 located in Figure 25) were excluded to give the best linear regression line. R'/R" substituents for excluded systems were Cl/NHC_6H_5, Cl/OC_2H_5, and Cl/$NHCOCH_3$. All three systems had Cl substituents for R'. Substituents for R" were substituted amine and ethoxy substituents.

The SOMO energy versus the experimental reduction potential plots are given in Figure 29. Linear regression data taken from the analysis demonstrated to have the best correlation coefficient value out of the parameters examined. With all 12 points included in the regression analysis, a correlation coefficient of 0.277 was obtained. With three points excluded (corresponding to systems 1, 10, and 11) a correlation coefficient of 0.908 was obtained giving the best fit. Substituents for excluded values were: for R', H, CH_3, and Cl, and for R", two systems substituted with H and one with NHC_6H_5.

Electronegativity versus reduction potential plots are located in Figure 30. A correlation of 0.527 was obtained when all twelve data points were included in the regression analysis. A correlation coefficient of 0.809 was obtained when the same three points excluded from the chemical hardness regression analysis (reduction potentials/systems excluded were -0.272/3, -0.192/7, and -0.165/8) were excluded. R'(R") substituents corresponded to Cl(NHC_6H_5, Cl(OC_2H_5), and Cl($NHCOCH_3$). Again, out of all possibilities, extraction of these systems gave the best fit linear regression line.

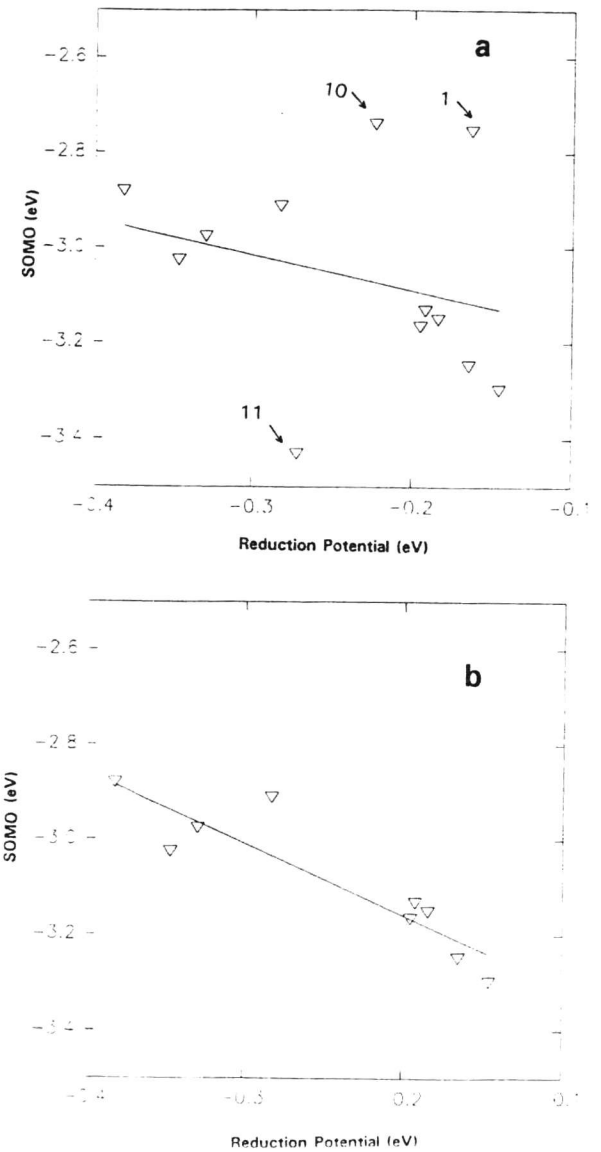

Figure 29. Plots of SOMO energies vs. reduction potentials for disubstituted 1,4-naphthaquinone systems (1-12, Figure 25). The plot in a is obtained by performing the regression analysis on all 12 points. The plot in b is obtained by excluding the points indicated by the arrows in a.

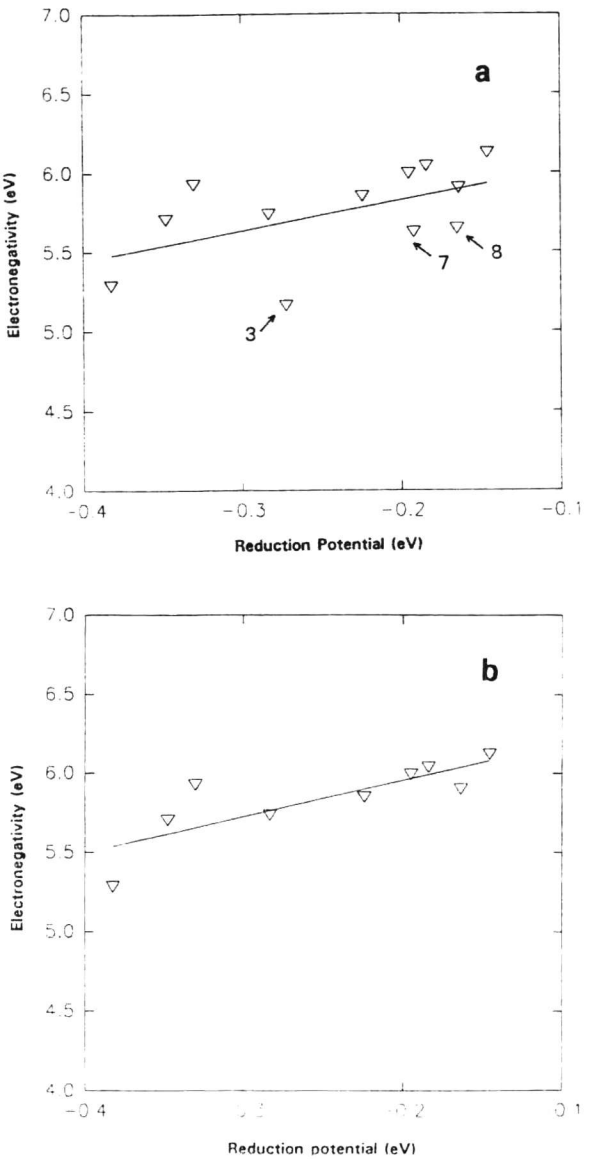

Figure 30. Plots of electronegativity vs. reduction potential for disubstituted 1,4-naphthaquinone systems (1-12, Figure 25). The point in a is obtained by performing the regression analysis on all 12 points. The plot in b is obtained by excluding the points indicated by the arrows in a.

All linear regression data is located in Table 15. The data include slope, intercept, and the correlation coefficient for the line fit. From parameters investigated, linear regression data demonstrated that better correlations could be obtained when some systems were excluded from the analysis.

The analysis presented here demonstrates how theoretical approaches can be useful in making predictions about the chemical reactivity of quinone-type systems.

TABLE 15. Summary of linear regression data computed for the 1,4-napthaquinone systems.

Parameter (# of pts)	Slope	Intercept	r[a]
η (12)	1.30	4.42	0.411
(9)	1.21	4.47	0.725
ΔH_{rxn} (12)	-20.6	-58.6	0.567
(9)	-22.1	-58.9	0.879
LUMO (12)	-0.58	-1.78	0.400
(9)	-1.11	-1.96	0.820
SOMO (12)	-0.75	-3.24	0.277
(9)	-1.51	-3.46	0.908
χ (12)	1.93	6.21	0.527
(9)	2.31	6.42	0.809

[a]r is the correlation coefficient obtained from the linear regression analysis.

IV. CONCLUSION

This study demonstrated how theoretical approaches may be useful in predicting the relative reactivities of reductively-activated quinones not readily amenable to experimental investigation. Adriamycin and daunomycin, two complex anthraquinones, are two such antitumor quinones known to undergo reductive activation to produce highly reactive species that immediately participate in electron-transfer reactions.[37] These electron-transfer reactions are believed to be responsible for the highly undesirable dose-dependent side effect (i. e. cardiotoxicity).

In an attempt to further understand the reactivity of anthracyclines, several quinones (part of the anthracycline pharmacophore) were used as model systems, to mimic one possible mechanism of anthracycline bioreduction. Model systems investigated in this study were 1,4-benzoquinone (and its imine and diimine analogs), 1,4-naphthaquinone, hydroxy-naphthaquinone, dihydroxy-naphthaquinone (and its imine analog). Parent compounds (benzoquinone and naphthaquinone) were compared with their imine and diimine analogs. Benzoquinone, naphthaquinone, hydroxy-naphthaquinone, and dihydroxy-naphthaquinone were compared with each other.

The reduction intermediates of the four quinone systems were compared to determine which system would ultimately yield the most reactive product(s) of reductive activation. After comparing the relative electronegativity of each redox state of the four systems, the following decreasing orders of

electronegativity were observed: Q, I>II>III>IV; $Q^{\cdot-}$, IV>III>II>I; $QH^{\cdot}$, I>III>IV>II; QH^{-}, IV>III>II>I; and QH_2, II>III>I>IV. For all four quinone systems, electronegativity and chemical hardness data suggested that QH^{-} and $Q^{\cdot-}$, respectively were the most reactive intermediates of reduction activation.

The effect of oxygen replacement by either imine or diimine substituents on the quinone systems, in general, made reactivity higher. This suggests that the activated forms of the imine and diimine analogs should be more reactive when compared to their parent counterparts. The higher reactivity predicted by the calculations strongly suggest that 5-iminodaunomycin should show more cardiotoxicity and the experimental observation of reduced toxicity for 5-iminodaunomycin must be due to other factors and/or a different mechanism and not because 5-iminodaunomycin can not be reduced or oxidized as efficiently as daunomycin.

The reduction potential of quinones have been cited as molecular descriptors in determining antitumor activity.[105] Reduction potenial has been directly related to the electronic HOMO-LUMO energy gap (i. e. absolute hardness).[83] In light of this, a linear regression analysis investigation was conducted to determine if the electronic parameters (absolute hardness, electronegativity, SOMO energies, and LUMO energies) calculated in this study would correlate well with experimental reduction potentials. Reaction enthalpy data for the electron attachment to Q were also correlated with the experimental reduction potentials. Data from regression analysis showed that

correlation coefficients were reasonably high (r values ranged from 0.73-0.91). In most cases, SOMO energies, reaction enthalpy values, and LUMO energies, decreased with increasing reduction potentials and electronegativity and chemical hardness values increased with increasing reduction potentials.

Hodnett and coworkers had determined the correlation between reduction potentials and antitumor activity.[83] They reported that the reduction potential threshold for desirable biological activity was $\geq$ -0.200 V (activity increasing with increasing reduction potential). But, they found that while desirable biological activity increased, toxicity is increased.

Parameters computed from the molecular orbital energies, electronegativity and absolute hardness, indicated that $QH^{\cdot}$ (in most cases) gave the most reactive species for quinone and its imine and diimine analogs. This implies that this redox-state of the systems is the most likely to participate in electron-transfer reactions to molecular oxygen. When the reactivities of the parent compounds were compared to their derivatives, all derivative redox systems gave lower electronegativity and absolute hardness values. This suggests that the imine and diimine redox states are more reactive compared to their quinone counterparts and that these systems should be more efficient in electron transfer reactions.

In summary, this theoretical study has shown that: correlations of the AM1 calculated electronic parameters and experimental reduction potentials were reasonably good; reaction enthalpies, SOMO energies, LUMO energies

decreased with increasing reduction potentials; absolute hardness and electronegativity values increased with increasing reduction potentials; within a group of redox states, based on electronegativity, $QH^- > Q^{\cdot-} > QH_2 > QH^{\cdot} > Q$ was the order of reactivity; chemical hardness data suggest that $Q^{\cdot-}$ was the most reactive intermediate for each model system; higher reactivities were observed for redox states of the imine and diimine analogs; and, AM1 calculated electronic parameters presented no obvious reactivity trends for the four model systems.

An interesting observation worth consideration is that the electronegativity values, computed for the quinone systems, were comparable to the experimental value determined for O_2. This suggests that the quinone systems may effectively compete in electron transfer reactions which occur in the mitichondria and thereby disrupting normal physiological processes.

The information gathered in this study strongly suggests that various electronic properties can be used to establish relationships between the electronic properties of various quinones and their biological activities. Futhermore, the initial studies presented in this thesis warrant futher studies which may include: determination of the relative reactivities of anthraquinone redox states; direct correlations of calculated AM1 electronic parameters with biological activity; determination of the effects of solvation on the overall reactivity of the redox states; determination of the effects of different substituents on the overall reactivity of the redox states (for example, how =S

would fare as a possible newly-synthesized anthracycline derivative should be interesting), and so on.

V. REFERENCES

1 Nohl, H.; Jordon,W.; Youghman, R.J. *Adv. Free Rad. Biol. Med.* 1986, 2, 211.

2 Brockmann, H., *Fortsch, Chem. Org. Naturst.* 1963, 21, 121.

3 DiMarco, A.; Gaetini, M.; Dorigotti, L.; Soldatti, M.; Bellini, O. *Tumori*. 1963, 49, 203.

4 Arcamone, F.; Franceshchi, G; Penco, S.; Selva, A. *Tetra. Lett.* 1969, 13, 1007.

5 Bachur, N. R.; Gordon, S. L.; Gee, M. V. *Cancer Res.* 1978, 38, 1745.

6 Casazza, A. M. *Cancer Treat*. 1986, Rep. 70, 43.

7 Bachur, N. R.; Cradock, J. C. J. *Phar. Exp. Ther.* 1970, 175, 331.

8. Nakazawa, H.; Andrews, P. A.; Callery, P. S.; Bachur, N. R. *Biochem. Pharmac.* 1985, 34, 481.

9. Andrews, P. A.; Brenner, D. E.; Chous, F. T.; Kabo, H.; Bachur, N. R. *Drug Meta. Disp*. 1980, 8, 152.

10. Bachur, N. R.; Gordon, S. L.; Gee, M. V.; Kon, H. I. *Proc. Nalt. Acad. Sci. USA* 1979, 76, 954.

11 Schweitzer, B.A.; Egholm, M.; Koch, T.H. *J. Am. Chem. Soc*. 1992, 114, 242.

12 Gaudiano,G.; Frigerio, T.; Bravo, P.; Koch, T.H. *J. Am. Chem. Soc.* 1992, 114, 3107.

13 Fullerbach, D.; Nagel, G. A.; Seeber, S. eds. Adriamycin Symposium, S. Karger AG, Basel

14 Arcamone, F. *Doxorubicin Anticancer Antibiotics*, 1981, Academic Press: New York, Vol. 17, pp.1.

15 Young, R.C.; Ozols, R.F.; Myers, C.K. *New Engl. J. Med.* 1977, 305, 139.

16 Tan, C.; Tasaka, H.; Yu, K.P.; Murphy, L.; Karnofsky, D. *Cancer* 1967, 20, 333.

17 Von Hoff, D.D.; Lazard, D.W. *Am. Interm. Med.* 1979, 91, 710.

18 Gianni, L.; Zweir, J. L.; Levy, A.; Myers, C.E. *J. Biol. Chem.* 1985, 260, 6820.

19 Gianni, L.; Vigano, L.; Lanzi, L.; Niggaler, M.; Malatesta, V.J. *Nalt. Cancer Inst.* 1988, 80, 1184.

20 Bachmann, E.; Weber, E.; Zbinden, G. *Agents* 1975, 5, 383.

21 Lown, J. W. *Mol. Cell. Biol.* 1983, 55, 17.

22 Chaires, J. B. *Biophys. J.* 1983, 41, 286.

23 Fritzsche, H.; Triebel, H.; Chaires, J.B.; Dattagupta, N.; Crothers, D.L. *Biochem.* 1982, 21, 3940.

24 Phillips, D.R.; White, R.J.; Trist, H.; Callinone, G.; Dean, D.; Crothers, D.L. *Anticancer Drug Des*. 1990, 5, 21.

25 Quadrifoglio, F.; Crescenzi, V. *Biophys. Chem*. 1974, 2, 64.

26 Xodo, L.E.; Manzini, G.; Ruggiero, J.; Quadrifolio, F. *Biopolymers* 1988, 27, 1839.

27 Van Boom, J. H.; Rich, A.; Wang, A. *Biochem*. 1990, 29, 2538.

28 Wang, A.; Ughetto, G.; Quigley, G.J.; Rich, A. *Biochem*. 1987, 26, 1152

29 Waring, M. *J. Mol. Biol*. 1970, 54, 247.

30 Chaires, J.B.; Dattagupta, N.; Crothers, D.M. *Biochem*. 1982, 21, 3933.

31 Sinha, B.K.; Sik, R.H. *Biochem. Pharmacol*. 1980, 29, 1867.

32 Fetsy, B.; Daune, M. *Biochem*. 1973, 12, 4827.

33 Wheeler, C.; Radar, R.; Kessel, D. *Biochem. Pharmacol.* 1982, 31, 2691.

34 Hickman, J.; Chahwala, S. B.; Thompson, M. G. *Adv. Enzym. Reg*. 1985, 24, 263.

35 Halliwell, B.; Gutteridge, J. M. C. *Free Radicals in Biology and Medicine* 1987, 2nd ed., Clarendon Press, 8, pp. 489.

36 Powis, G. *Free Rad. Biol.* 1989, 63, 105.

37 Bachur, N.R.; Gordon, S. L.; Gee, M.V. *Can. Res*. 1978, 38, 1745.

38 Handa, K.; Sato, S. *Gann* 1975, 66, 43.

39 Bachur, N.R.; Gordon, S.L.; Gee, M.V. *Mol. Pharmacol.* 1977, 13, 901.

40 Sato, S.; Iwaizumi, M.; Handa, K.; Tamura, Y. *Gann* 1977, 68 603.

41 Schreiber, J.; Mottley, C.; Sinha, B.K.; Kalyanaraman; Mason, R. P. *J. Am. Chem. Soc.* 1987, 109, 348.

42 Svingen, B.A.; Powis, G. *Arch. Biochem. Biophys.* 1981, 209, 119.

43 Kalyanaman, B.; Preez-Reyes, E.; Mason, R. P. *Biochem. Biophys. Acta.* 1980, 630, 119.

44 Nakazawa, H.; Andrews, P. A.; Callery, P. S.; Bachur, N.R. *Biochem. Pharmacol.* 1985, 34, 481.

45 Sawyer, D. T.; Roberts, J. L.; Calderwood, T. S.; Tsuchiya, T.; Stamp, J. J. *Oxygen Rad. & Their Scavenger Systems*, 1986, Vol. 1, pp. 8.

46 Mimnaugh, E. G.; Gram, E. G.; Trush, M. A. *J. Pharmacol. Exp. Ther.* 1983, 226, 806.

47 Winterbourn, C. C.; Sutten, H. C. *Arch. Biochem. Biophys.* 1984, 235, 116.

48 Moore, H. W.; Czerniak, R. *Med. Res. Rev.* 1981, 1, 249.

49 Sinha, B.K.; Chignell, C. F. *Chem. Biol. Interact.* 1979, 28, 301.

50 Scheulen, M. E.; Kappus, H.; Nienhaus, H.; Schmidt, C. G. J. *J. Can. Res. Clin. Oncol.* 1982, 103, 39.

51 Sinha, B. K. *Chem. Biol. Interact*. 1980, 30, 67.

52 Moore, H. W. *Science*, 197, 527, 1977.

53 Koch, T. H. ; Fisher, J. *J. Am. Chem. Soc*. 1983, 105, 7187.

54 Ramakrishnan, K.; Fisher, J. *J. Med. Chem*. 1986, 29, 1215.

55 Bartoszek, A.; Wolf, C. R. *Biochem. Phar*. 1992, 43, 1449.

56 Manoney, R. P.; Fretwell, P. A.; Demordis, S. H.; Mauldin, R. K.; Deson, O.; Koch, T. H. *J. Am. Chem. Soc*. 1992, 114, 186.

57 Thomas, C . E.; Aust, S. D. *Arch. Biochem. Biophys*. 1986, 248, 684.

58 Bachmann, E.; Weber, E.; Zbinden, G. *Agents Actions* 1975, 5, 383.

59 Revis, N. W.; Marcusic, N. *Exp. Mol. Pathol*. 1986, 31, 440.

60 Doroshow, J. H.; Davies, K. *J. Biol. Chem*. 1986, 261, 3068.

61 Doroshow, J.H.; Davies, K.J. *J. Biol. Chem*. 1986, 261, 3068.

62 Mimnaugh, E. G.; Trush, M. A.; Gran, T. E. *Biochem. Pharmacol*. 1983, 30, 2797.

63 Daugherty,; Wheat, M.; Conley, E.; Loggins, L.; Durant, J. R. *Proc. Am. Assoc. Can. Res*. 1982, 23, 171.

64 Sinha, B.K. *Chem. Biol. Interact*. 1989, 69, 293.

65 Banfi, P.; Parolini, O.; Lazi, C.; Gambetta, R. A. *Biochem. Phar*. 1992, 43, 1521.

66 Benchekrown, M. N., Robert, E. *J. Anal. Biochem*. 1991, 201, 326.

67 Lin, T.; Liu, G. *Biochem. Biophys. Res. Comm*. 1989, 178, 207.

68 Lown, J. W.; Chen, H. H-; Plambeck, J. A.; Acton, E. M. *Biochem. Phar*. 1979, 28, 2563.

69 Myers, C. E.; Muindi, R. F.; Zweier, J.; Sinha, B. K. *J. Biol. Chem*. 1987, 262, 11571.

70 Tony, G. L.; Henry, D. W.; Acton, E. M. *J. Med. Chem*. 1979, 22, 36.

71 Richardson, C. L.; Schulmen, G. L. *Biochim. Biophys. Acta*. 1981, 652, 55.

72 Zbinden, G.; Brandle, L.; C. Chem. Rep. 1975, 59, 707.

73 Bird, D. M.; Boldt, M.; Koch, T. H. *J. Am. Chem. Soc*. 1987, 109, 4046.

74 Weller, K.; Schutz, H.; Katenkamp, U. *Studia Biophysica* 1984, 104, 37.

75 Tong, G. L.; Henry, D. W.; Acton; E. M. *J. Med. Chem*. 1979, 22, 36.

76 Glazer, R. I.; Hartman, K. D.; Richardson, C. L. *Can. Res*. 1982, 42, 117.

77 Powis, G. *Phar. Ther*. 1987, 35, 57.

78 Bird, D. M.; Boldt, M.; Koch, T. H. *J.Am. Chem. Soc*. 1987, 109, 4046.

79 Lin, A.; Pardini, R.S.; Cosby, L. A.; Lillis, B. J.; Shansky, C. W.; Sartorelli, A. C. *J. Med. Chem*. 1973, 16, 1268.

80 Hodnett, E. M.; Wongwiechintana, C.; Dunn, W. V.; Marrs, P. *J. Med. Chem*. 1983, 26, 570.

81 Koopman, T. *Physica* 1934, 1, 104.

82 SigmaPlot Scientific Graphing System, 1990, Version 4.02, (c) Jandel Corp.

83 Ranghino, R.; Tosi, C. *Theochem* 1987, 151, 287.

84 Gianni, L.; Corden, B. J.; Myers, C.E. *Rev. Biochem. Toxicol.* 1983, 5, 2.

85 Dewar, M.J.; Zoebisch, E.G.; Healy, E.G.; Steward, J.J.P. *J. Am. Chem. Soc.* 1985, 107, 3902.

86 Healy, E.F. Univ. Texas at Austin, Personal Communication.

87 Parr, R.G.; Pearson, R. G. *J. Am. Chem. Soc.* 1983, 105, 7512.

88 Pearson, R.G. *J. Chem. Ed.* 1987, 64, 561.

89 Thiel, W. *Tetrahedron* 1988, 44, 7393.

90 Stewart, J. J. P. *J. Comp. Aided Mol. Des.* 1990, 4, 1.

91 Liotard, D. A.; Healy, E. F.; Ruiz, J. M.; Dewar, M. J. S. *QCPE Program 506*, Indiana University, Bloomington, IN 47405.

92 Stewart, J. J. P. *Quantum Chem. Program Exchange Program, No. 455*, Dept. Chem., Indiana Univ., Bloomington, IN 47405.

93 PCMODEL program, 1989, Version 3.0 Indiana, Univ. Bloomington IN 47405.

94 Keywords used in this investigation (and their meanings) were: GRADIENTS (all gradients were printed on calculation); ENPART (energy was partitioned into components); PRECISE (criteria of calculation was increased by 100); POWELL (calculation was optimzed based on Powell parameters);

95 Pearson, R.G. *J. Am. Chem. Soc.* 1985, 107, 6801.

96 Parr, R. G.; Donnelly, R.A.; Levy, M.; Palko, W. G. *J. Chem. Phys.* 1978, 68, 3801.

97 Huheey, J. E. *J. Phys. Chem.* 1965, 85, 148.

98 Berkowitz, M.; Ghosh, S. K.; Parr, R. G. J. Am. Chem. Soc. 1985, 107, 6811.

99 Fischer, H.; Kollmar, H. *Theor. Chim. Acta*. 1970, 16, 1631.

100 Bischof, P. J. *J. Am. Chem. Soc*. 1976, 98, 6844.

101 Phillips, D. R.; Crothers, D. M. *Biochemistry*, 1987, 25, 7355.

102 Straney, D. C.; Crothers, D. M. *Biochemistry*, 1987, 26, 1987.

103 Rizzo, V.; Sacchi, N.; Menozzi, M. *Biochemistry*, 1989, 28, 274.

104 Brey, W. S. *"Physical Chemistry and lis Biological Application"*, 1978, Academic Press, New York, pp 233.

105 Ahmad, J.; Astin, K. B. *Revue Roumainide Chimie* 1985, 33, 321.